JOINT FREQUENCY/POWER UPDATE ALGORITHMS FOR SELF-ORGANIZING FEMTOCELL NETWORKS

by

Oğuzhan Sevim

B.S., Electrical and Electronics Engineering, Boğaziçi University, 2016

Submitted to the Institute for Graduate Studies in
Science and Engineering in partial fulfillment of
the requirements for the degree of
Master of Science

Graduate Program in Electrical and Electronics Engineering
Boğaziçi University

2019

JOINT FREQUENCY/POWER UPDATE ALGORITHMS FOR SELF-ORGANIZING FEMTOCELL NETWORKS

APPROVED BY:

Prof. Mehmet Akar ..... (Thesis Supervisor)

Prof. Emin Anarım .....

Assist. Prof. Onur Cihan .....

DATE OF APPROVAL: 23.07.2019

ACKNOWLEDGEMENTS

I would first like to thank my advisor Prof. Mehmet Akar for his support, advice, and knowledge. Throughout the whole period of my master's studies, his guidance has immeasurably widened my mind and knowledge in many aspects.

I also would like to thank the members of my thesis committee, Prof. Emin Anarım and Assist. Prof. Onur Cihan, for participating the defence of this thesis, and for their supportive evaluations.

My sincere gratitude goes to my colleague and friend Halil Yiğit Öksüz for his valuable support and contributions in different studies within the scope of this thesis.

I am also grateful for the funding that I have received from TÜBİTAK Project 115E397.

Lastly, my very special thanks goes to my friend Kübra Eşmeli and to my family for their precious support and love.

ABSTRACT

JOINT FREQUENCY/POWER UPDATE ALGORITHMS FOR SELF-ORGANIZING FEMTOCELL NETWORKS

Heterogenous networks are resorted as one of the most promising ways for meeting the rapidly increasing data demand. As the smallest members of heterogenous networks, femto base stations also carry a huge potential for increasing the service quality in indoor areas. However, their unplanned deployment by the end users increases the possibility of having dense femtocell networks with unknown topologies. Therefore, self–organizing methods have great importance in resource allocation of femtocell networks.

In this thesis, power and frequency allocation problems are studied for OFDMA femtocell networks. First, we present a power update algorithm for the general wireless networks as an alternative for a well known power control algorithm from the literature. Then, this algorithm and another power control algorithm from the literature are extended for the OFDMA femtocell networks. As opposed to the previous versions, which are applicable only in networks where each base station can have at most one user, the extended algorithms can be used by base stations that have more than one user. Additionally, a frequency allocation scheme is developed in order to increase the maximum achievable SINR in femtocell networks. Furthermore, by merging this scheme with the proposed power update algorithms, we present two joint frequency/power update algorithms with increased performance. Convergence and optimality analyses of all the proposed algorithms are carried out and illustrated with numerical results.

ÖZET

ÖZÖRGÜTLEMELİ FEMTO HÜCRE AĞLARI İÇİN TÜMLEŞİK FREKANS/GÜÇ ATAMA ALGORİTMALARI

Hızla yükselen veri talebini karşılamak için başvurulan yöntemler arasında heterojen ağlar önemli bir yer tutmaktadır. Heterojen ağların en küçük üyeleri olan femto baz istasyonları, ev ve ofis gibi kapalı yerlerdeki servis kalitesini artırmaya yönelik büyük bir potansiyel arz ederler. Femto hücrelerin kurulumu kullanıcılar tarafından plansız bir şekilde yapıldığından, femto hücre ağlarının yoğun ve bilinmeyen bir topolojiye sahip olması kaçınılmaz hale gelmektedir. Bu nedenle, femto hücrelerin kaynak atama işlemini özörgütlemeli bir şekilde yapması gerekmektedir.

Tez kapsamında ilk olarak, genel kablosuz haberleşme ağlarında kullanıma uygun bir güç kontrol algoritması önerilmiştir. Bu algoritma, literatürde iyi bilinen bir güç kontrol algoritmasına alternatif olarak ortaya konulmuştur. Devamında, önerilen bu algoritma ve literatürden alınan onaylaşım temelli bir başka güç kontrol algoritmasının çoklu kullanıcılara sahip baz istasyonlarından oluşan OFDMA tabanlı femto hücre ağları için uyarlanması sonucu iki güç kontrol algoritması geliştirilmiştir. Geliştirilen bu algoritmalar erişilebilir en yüksek SINR değerini artıran bir frekans atama kuralıyla birleştirilmiş ve iki farklı tümleşik frekans/güç atama algoritması elde edilmiştir. Tez kapsamında önerilen algoritmaların yakın- sama ve optimalite analizleri yapılmış, yapılan kuramsal sonuçlar benzetim çalışmalarıyla desteklenmiştir.

TABLE OF CONTENTS

LIST OF FIGURES

LIST OF SYMBOLS

a_{ij}	Weight of edge (j,i)
$\mathbf{A}$	Adjacency matrix for graph
$\mathbf{B}$	Diagonal matrix with update constants
$d_{i,j}$	Physical distance between user i and base station j
E	Set of edges for a graph
$f_{ij}(t)$	Connection weights between base station i and j at time t
$f_m^s(t)$	Self weight of subchannel s of base station m at time t
$\tilde{f}_m^s(t)$	Intra–cell connection weights of base station m at time t
g_{ij}	Channel gain between user i and base station j
G	A graph
h_{ij}	Normalized channel gain between user i and base station j
$\mathbf{H}$	Normalized channel gain matrix
$I_i(t)$	Interference experienced by user i at time t
$\mathcal{I}$	Set of transmitter/receiver pairs
$\mathbf{I}$	Identity matrix
$\mathbf{I_d}(t)$	Diagonal matrix with interference values at time t
K_m	Number of users served by base station m
$\mathcal{K}_m$	Set of users served by base station m
l_{ij}	Element of $\mathbf{L}$ on row i, column j
$\mathbf{L}$	Laplacian matrix
M	Number of transmitter/receiver pairs
$\mathcal{M}$	Set of all base stations
M_f	Number of femto base stations
N_i	Set of close neighbors of base station i
$\mathbf{N}$	Inverse of diagonal matrix with number of close neighbors
$p_i(t)$	Transmission power of base station i at time t
p_i^*	Transmission power of base station i when consensus is reached
$p_m^s(t)$	Transmission power of base station m on subchannel s at time t

$\mathbf{p}(t)$	Power vector at time t
$\mathbf{p}^*$	Power vector when consensus is reached
$\widetilde{\mathbf{p}}(t)$	The vector that contains transmission powers on all the active subchannels used by all FBSs at time t
$r(\cdot)$	Spectral radius function
$\mathbb{R}$	Set of real numbers
S	Number of available OFDMA subchannels
$\mathcal{S}$	Set of available OFDMA subchannels
T_s	Sampling period
U	Total number of actively used subchannels
U_m	Number of subchannels actively used by base station m
$\mathcal{U}_m$	Set of subchannels actively used by base station m
V	Set of nodes for a graph
$x_i(t)$	State of node i at time t
$\mathbf{x}(t)$	State vector at time t
α	Path loss exponent
β_i	Update constant of base station i
γ	Desired SINR value
γ^*	SINR value when consensus is reached
$\Gamma_i(t)$	SINR value of user i at time t
$\Gamma_{i,ref}(t)$	Reference SINR value of user i at time t
$\Gamma_{m,ave}(t)$	Average SINR of the users of base station m at time t
$\Gamma_m^s(t)$	SINR of the downlink signal transmitted by BS m on subchannel s at time t
$\mathbf{\Gamma}(t)$	Vector of SINR values at time t
$\widetilde{\mathbf{\Gamma}}(t)$	Vector that contains the SINR values on active subchannels of entire femtocell network at time t
η_i	Normalized thermal noise experienced by user i
$\boldsymbol{\eta}$	Vector of normalized thermal noise
$\rho_{m,k}^s$	Subchannel assignment variable indicating connection status between base station m and user k on subchannel n

σ_i	Thermal noise experienced by user i

LIST OF ACRONYMS/ABBREVIATIONS

2G	Second Generation
3G	Third Generation
BS	Base Station
CQI	Channel Quality Information
FBS	Femto Base Station
FUE	Femto User Equipment
HetNets	Heterogeneous Networks
JFPUA-I	Joint Frequency/Power Update Algorithm one
JFPUA-II	Joint Frequency/Power Update Algorithm two
LTE	Long Term Evolution
MBS	Macro Base Station
MUE	Macro User Equipment
OFDMA	Orthogonal Frequency Division Multiple Access
PCA	Power Control Algorithm
PUA-I	Power Update Algorithm one
PUA-II	Power Update Algorithm two
PUA-III	Power Update Algorithm three
SINR	Signal to Interference plus Noise Ratio
UE	User Equipment
WiMAX	Worldwide Interoperability for Microwave Access

1. INTRODUCTION

Global mobile data traffic is expected to be five times higher in 2024 compared to 2018 [1]. Small cells, also known as low–power base stations, have been used as one of the promising ways to meet this exponentially increasing data demand. From the largest connection capacity to the lowest, these low–power base stations are named as micro/pico/femto base stations. A network that includes low–power stations with macro base stations (MBSs) is called a multi–tier network where each tier consists of the collection of all similar base stations (BS). These type of networks, which include more than one type of BS, are also classified as Heterogeneous Networks (HetNets). In terms of spectral efficiency, HetNets are superior than conventional (homogenous) cellular networks which consist solely of macro base stations [2]. An example of a three–tier HetNet is shown in Figure 1.1.

Femto base stations (which may be referred as femtocells in the rest of this thesis), the latest and the smallest member of the low–power base stations, are designed to provide service for the indoor areas (houses, offices, etc.). They are purchased and deployed by the end users like the WiFi access points. A single femtocell can provide service up to 8 user equipments [3]. Deployment of a new femto base station (FBS) into coverage area of an existing macro base station can provide faster connection (higher data rate) for the users who suffer from low service quality. Thanks to the decreased cell radius and the transmitter to receiver distances, users can have high received signal strength. Ultimately, by using these access points appropriately, the overall capacity and data throughput of a given network can be increased.

Depending on the air interference technologies, different kinds of femtocells are in use (e.g., 2G, 3G, and OFDMA femtocells) [4]. Among those, OFDMA (Orthogonal Frequency Division Multiple Access) based femtocells are the ones that is suitable for LTE and WiMAX technologies which are likely to be used mostly in near future. Before femtocell technology becomes widespread, interference management (along with other issues like synchronisation and security) still stands among the major technical challenges that need to be solved. In an OFDMA based, two–tier femtocell network, interferences may occur between cells of the

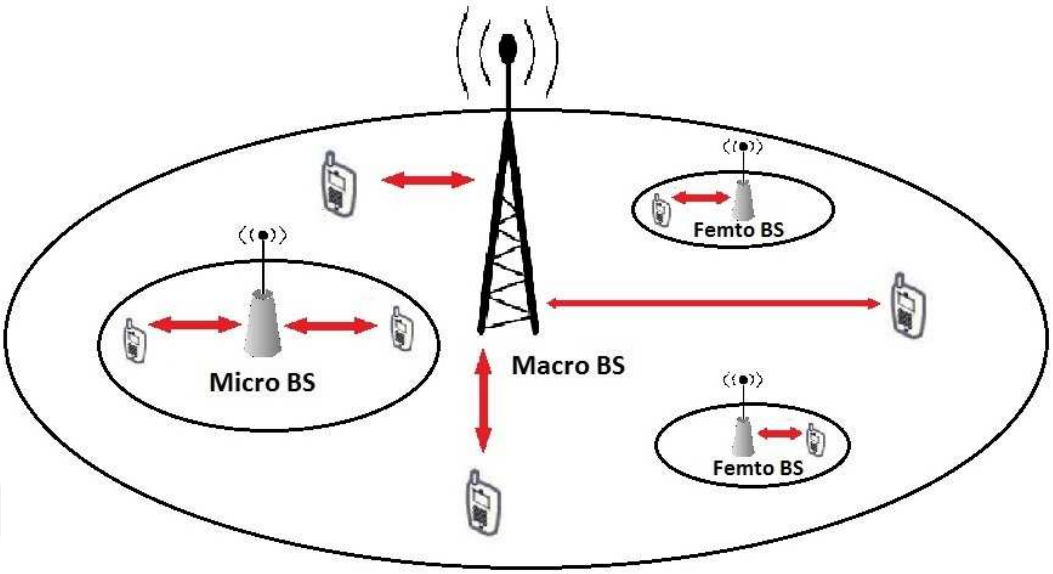

Figure 1.1. An example network with three tiers.

same tier (co–tier) or the cells of different tiers (cross–tier). Since a base station does not assign a subchannel (subcarrier) to more than one user equipment (UE), by the orthogonality of the OFDMA subcarriers (subchannels), interference between the users of the same cell is eliminated.

Based on portioning the available OFDMA subchannels, a two-tier network can be classified into two: split and shared spectrum setups [5]. In the split spectrum case, macro and the femto base stations use different OFDMA subcarriers, and cross–tier interference is almost completely eliminated [6]. However, reserving a certain part of available spectrum just for the femtocells can be costly due to the scarcity of available spectrum. When all available subchannels are used by both femtocells and macrocells (shared spectrum), we have higher spectral reuse. As a trade off, the interference management problem now includes dealing not only with co–tier interference but also the cross–tier interference.

Deployment of the femtocells is done by the end users with no cell planning of operators. The unplanned deployment of the femtocells makes the network have an unpredictable dynamic topology with the unknown number of base stations and users. It is also highly likely that distance between the femtocells of two neighbors may be less than a meter. The

possibility of having a huge number of agents with unknown locations, makes the network almost impossible to be controlled by a central decision maker in real life applications. In contrast, decentralized solutions, where the base stations control their own resources by using the information coming from their close neighbors, are much more realisable and require less computational effort [7].

Different techniques have been proposed and used for interference management in femtocell networks. Interference cancellation, which eliminates the interference after signal is received, is one of these methods [4]. Interference management of an OFDMA femtocell network can also be done by the control of transmission power levels, by frequency subchannel assignment, or by handover techniques.

In [8], a distributed frequency allocation algorithm is proposed for the OFDMA based, two–tier networks, and the algorithm is proven to be decreasing the spectrum usage for a desired quality of service. A macro user equipment (MUE) protective frequency allocation scheme is proposed in [9], where the MUEs vulnerable to femtocell interference are placed on a macro dedicated portion of the available spectrum according to the incoming Channel Quality Information (CQI). In [10], game theoretical approaches are used for the power control of the two–tier femtocell networks. With the aim of maximizing the total throughput of femto user equipments (FUEs), joint power/subchannel allocation algorithms were proposed in [11] and [12], where non–convex mixed-integer optimization problems were relaxed into convex versions.

A water–filling based power control algorithm has presented in [13] with the objective of maximizing the throughput/energy ratio in two–tier networks. With a similar objective function, a joint power/frequency allocation algorithm has been proposed in [14]. In order to make sure that cross–tier interferences experienced by MUEs are under a predefined level, a distributed downlink power control algorithm is proposed in [15] by using two major assumptions that there exists a unidirectional broadcast channel that carries information about the locations of MUEs from MBS to FBSs, and that FBSs are aware of their location.

The issue of fairness has been addressed in the literature in different works. [16] is one of the relatively early ones where the problem is regarded as a maximization of the total system capacity with the constraints that ensures the proportional fairness. However, the system model involves only a single base station, and the available OFDM subchannels are assumed to be used by at most one user equipment (UE). Therefore, under this model, co-tier interference does not exist. That makes the algorithm a little unpractical for the dense femtocell networks.

The early studies of Foschini and Miljanic [17] can be considered as one of the earliest autonomous power control algorithms that aim fairness. By imposing the same SINR target to all user equipments, they aim to achieve fairness in the network. In recent studies of Senel and Akar, such as [18] and [19], several consensus based power control algorithms have been proposed with the objective of achieving fairness. In [18], the proposed power control algorithm is analytically and numerically proven to be establishing the fairness among all the users in the femtocell network in terms of their SINR (Signal to Interference plus Noise Ratio) values. The other details of the algorithm given in [18], including stability, convergence rate, and optimality analysis, can be found in [20, 21].

1.1. Motivations of the Thesis

The power control algorithm proposed by Foschini–Miljanic [17] provides the same predetermined SINR for all receivers in a given network. However, as the major drawback of this algorithm, depending on the channel conditions, this predetermined target SINR value may not always be feasible. In order to set a feasible target value, channel conditions of the entire network should be known beforehand by a centralized unit. For the crowded networks, implementation of such an approach may not be possible, and there arises the need for a completely decentralized algorithm that erases the infeasibility issue.

In the study given in [18], Şenel–Akar have presented a consensus based power control algorithm which has proved to be providing fairness among the receivers of a network. However, in the network model used in this study, it is assumed that each base station has only one user equipment, and that all users equipments get service on the same frequency

channel. Since real life OFDMA base stations serves more than one user equipments on multiple subchannels, this algorithm needs to be modified for more realistic models.

Finally, the algorithms that are proposed as a result of the given motivations performs only power updates. By using them with a proper frequency allocation scheme, we aim to improve their performance.

1.2. The Contributions of the Thesis

Main contributions of this thesis can be listed as follows:

- A consensus based power update algorithm is proposed as a better alternative for the well known algorithm of Foschini-Miljanic given in [17].
- Optimality analysis of the networks consisting of transmitter/receiver pairs is carried out.
- A graph expansion method is proposed for the power control algorithm given in [18]. By using this method, 2 power update algorithms are presented for the OFDMA femtocell networks.
- In order to increase the maximum achievable SINR of a given OFDMA femtocell network, a frequency allocation scheme is derived. Additionally, by using this scheme, 2 joint frequency/power update algorithms are proposed.
- It is analytically and numerically shown that all five algorithms discussed above ensure fairness in the entire network when the underlying graph of the network is connected.

1.3. The Organization of the Thesis

The remaining chapters of this thesis are as organized follows: In Chapter 2, we first introduce some definitions and results from graph theory and consensus algorithms. Then, the background studies that inspired this thesis are briefly discussed.

In Chapter 3, a consensus based power update algorithm for the general wireless communication networks is introduced. Some theoretical analyses regarding the convergence and

optimality of the algorithm are presented. Additionally, simulation results of the algorithm are given.

For OFDMA femtocell networks, two power update algorithms are introduced in Chapter 4. Convergence analyses of the algorithms are carried out. Theoretical analyses are also illustrated with numerical results.

In Chapter 5, a frequency allocation scheme is proposed with the objective of maximizing the optimal SINR solution. Then, two joint frequency/power update algorithms are presented with their theoretical and numerical results.

Finally, in Chapter 6, some concluding remarks are given with some possible topics to be studied in future.

2. CONSENSUS PROBLEM AND PRIOR STUDIES

In this chapter, we first review basic concepts on graph theory and consensus algorithms. Then, prior works of Foschini–Miljanic and Şenel–Akar, which can be considered as the background studies of this thesis, will be discussed briefly.

2.1. Graph Theory

A graph is defined as a pair $G = (V, E)$, where $V = \{1, \ldots, n\}$ denotes the set of nodes (agents), and the set of edges (links between the agents) is given by E. $(i, j) \in E$ if there is an information flow from node i to node j. If the information links between the nodes are mutual (i.e., $(j, i) \in E$ is satisfied for all $(i, j) \in E$), then the corresponding graph is called to be undirected, otherwise it is directed. Examples of undirected and directed graphs with 3 nodes are shown in Figure 2.1. The arrows used in Figure 2.1(b) represent the directed information flow between nodes, where plain lines show bidirectional information exchange between the nodes of undirected graph in Figure 2.1(a).

The adjacency matrix of a graph can be defined as $\mathbf{A} = \left[a_{ij}\right]$, where $a_{ij} > 0$ if $(j, i) \in E$, while $a_{ij} = 0$ for all $(j, i) \notin E$. The element a_{ij} of the matrix $\mathbf{A}$ corresponds to the weight of the edge (j, i). Also, for an equally weighted graph, non–zero a_{ij} elements can be taken as 1. With these definitions, the Laplacian matrix can be defined as $\mathbf{L} = \left[l_{ij}\right] \in \mathbb{R}^{n \times n}$, where $l_{ii} = \sum_{j \neq i} a_{ij}$, and $l_{ij} = -a_{ij}$ for all $i \neq j$. Then, sum of all elements in any row of a Laplacian matrix is equal to zero.

An undirected graph (i.e., $a_{ij} = a_{ji}$ for all $i, j \in V$) is said to be connected if there exists a path between any chosen pair of nodes. For an undirected graph, the following two statements hold true [22]:

- $\mathbf{L}$ is symmetric positive semidefinite, and all of its nonzero eigenvalues are positive.
- 0 is a simple eigenvalue of $\mathbf{L}$ if and only if the graph is connected.

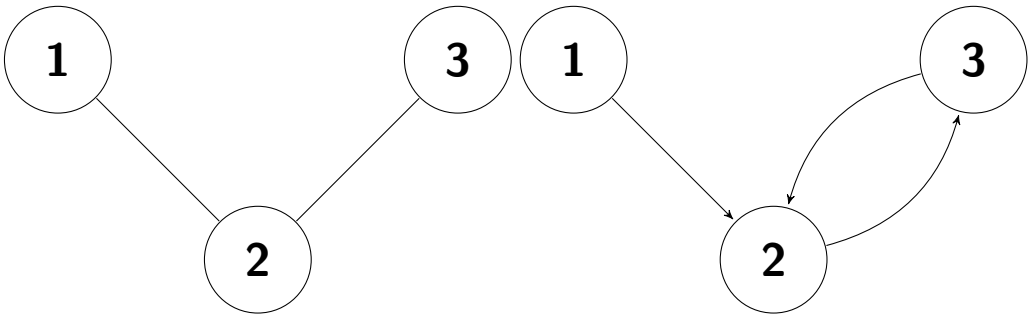

(a) An undirected graph (b) A directed graph

Figure 2.1. Example graphs with 3 nodes

2.2. Consensus Algorithms

This section provides some brief information about a particular type of consensus algorithm that will be used in the later chapters. The main motivation behind the consensus algorithms is to make desired states of a given system converge to a common equilibrium point when the given system can not be controlled by a centralized unit. Consensus algorithms are widely used in various application areas like formation control [23], smart grids [24], blockchain technology [25], wireless communication networks, etc. For a time–invariant network, the most common continuous–time consensus algorithm can be given as [26]

$$\dot{x}_i(t) = -\sum_{j=1}^{n} a_{ij}(x_i(t) - x_j(t)), \;\; i = 1, \ldots, n, \tag{2.1}$$

where coefficient a_{ij} is the element on row i and column j of adjacency matrix of corresponding graph. When there is an information flow from agent j to agent i, $a_{ij} > 0$ holds, otherwise $a_{ij} = 0$. By using the Laplacian matrix defined in Section 2.1, this equation can be written in vector form as

$$\dot{\mathbf{x}}(t) = -\mathbf{L}\mathbf{x}(t). \tag{2.2}$$

When the corresponding graph of the network is undirected (i.e., $a_{ij} = a_{ji}, i, j \in V$) and connected, 0 is a simple eigenvalue of $\mathbf{L}$ with the corresponding eigenvector of $\mathbf{1}$, where $\mathbf{1}$ is

a column vector of ones with length of n. Then, $\dot{\mathbf{x}}(t) = 0$ holds only when $\mathbf{x}(t) = \alpha\mathbf{1}$ for any scalar α. Therefore, we can conclude that the system (2.1) is at equilibrium state only when $x_i(t) = x_j(t)$ holds for all $i, j \in V$

2.3. Related Power Control Algorithms

In this section, we will discuss two power control algorithms proposed respectively by Foschini–Miljanic and Şenel–Akar. Both algorithms are designed to establish fairness in terms of the data rate provided to the user equipments of a given network. These algorithms constitute a basis for the algorithms proposed in this thesis where they are improved/extended in terms of feasibility and practicality.

2.3.1. Power Control Algorithm of Foschini–Miljanic

The study of Foschini–Miljanic [17] can be considered as one of the earliest distributed power control algorithms in literature. Their work considers the downlink case of a wireless communication network with M transmitter/receiver pairs, where the set of all pairs is denoted by $\mathcal{I} = \{1, 2, \ldots, M\}$. If $p_i(t)$ denotes the transmission power of BS i, then the SINR of its users can be calculated by

$$\Gamma_i(t) = \frac{p_i(t)}{\sum\limits_{j \in \mathcal{I}, j \neq i} h_{ij} p_j(t) + \eta_i} = \frac{p_i(t)}{I_i(t)}, \tag{2.3}$$

where $h_{ij} = g_{ij}/g_{ii}$ and $\eta_i = \sigma_i/g_{ii}$. Here, g_{ij} is the downlink channel gain between UE i and interfering BS j, $\sigma_i > 0$ denotes the power of thermal noise received by UE i, and $I_i(t)$ can be considered as the value of normalized interference on UE i at time t. With this notation, power control algorithm given in [17] can be written as

$$\dot{p}_i(t) = -\beta \left(1 - \frac{\gamma}{\Gamma_i(t)}\right) p_i(t), \forall i \in \mathcal{I}. \tag{2.4}$$

Here, β is a positive update constant and γ is a predefined SINR value that is aimed by all the BSs. By using the algorithm given in (2.4), BS i updates its transmission power until

SINR of UE i reaches the predefined target value γ (i.e., $\dot{p}_i(t) = 0$ when $\Gamma_i(t) = \gamma$). When this target value is reached by all UEs (i.e., $\Gamma_i = \gamma$, $\forall i \in \mathcal{I}$), (2.3) can be written as

$$\frac{p_i(t)}{\gamma} = \sum_{j \in \mathcal{I}, j \neq i} h_{ij} p_j(t) + \eta_i, \tag{2.5}$$

which, in vector form, leads to

$$(\tfrac{1}{\gamma}\mathbf{I} - \mathbf{H})\mathbf{p}^* = \boldsymbol{\eta}, \tag{2.6}$$

where $\mathbf{I}$ is $M \times M$ identity matrix, $\mathbf{H}$ is an M-dimensional square matrix with zero diagonal and positive $\left[h_{ij}\right]$ values on off-diagonals, $\boldsymbol{\eta}$ denotes an M-dimensional vector containing η_i values which are non–negative.

In order to find a feasible (non–negative power vector) solution to (2.6) for all possible non–negative $\boldsymbol{\eta}$ vectors, $(\frac{1}{\gamma}\mathbf{I} - \mathbf{H})$ should be a monotone matrix. Since this matrix has non–positive off-diagonal entries, being monotone equivalently means being an M–matrix [27, 28]. Thus, we can conclude that for (2.6) to have a feasible solution, γ needs to be set below a upper limit such that $\frac{1}{\gamma} > r(\mathbf{H})$, where $r(\mathbf{H})$ denotes the spectral radius of the matrix $\mathbf{H}$. Note that it is hard to make the correct choice of γ in a distributed manner since the upper limit of γ depends on channel gains of the entire network. For a predefined γ, the network is not always feasible to have a solution. In Section 3, we propose a consensus based power update algorithm (PUA-I) which eliminates this feasibility issue.

2.3.2. Power Control Algorithm of Şenel–Akar (PCA)

Reconsider the downlink case of a wireless communication network model with M transmitter/receiver pairs (base station/user), where $\mathcal{I} = \{1, 2, \ldots, M\}$. For this network, where the SINR of UE i is given by (2.3), a consensus based power control algorithm (PCA) has been proposed by Şenel–Akar in [18] as follows:

$$\dot{p}_i(t) = -\beta_i \frac{\Gamma_i(t)}{p_i(t)} \left[f_{ii}(t)\Gamma_i(t) - \sum_{j \in N_i} f_{ij}(t)\Gamma_j(t) \right], \quad \forall i \in \mathcal{I}. \tag{2.7}$$

Here, β_i is a constant that controls the update speed of $p_i(t)$, where N_i denotes the set of close neighbors of BS i. Also, $f_{ii}(t)$ and $f_{ij}(t)$ are the defined as connection weights. When the underlying communication graph is connected, it is proven that PCA converges to a fair solution $\mathbf{\Gamma}^*$, where $\Gamma_i^* = \Gamma_j^*$ holds $\forall i, j \in \mathcal{I}$. Detailed analysis of PCA, including stability, convergence rate, and optimality analysis, can be found in [18, 20, 21].

PCA given in (2.7) is applicable for the networks where all BSs have a single UE to serve. However, in real life OFDMA femtocell networks, there exist multiple subchannels and a BS is more likely to have more than one UE. Also by its nature, a joint frequency/power allocation problem should have multiple subchannels. In order to make the given PCA more realistic for real life applications and more practical for joint resource allocation problems, PCA is modified so that it ensures the global consensus in OFDMA femtocell networks where BSs serve more than a single UE. This new power update algorithm (PUA-III) is introduced in Section 4.3, with its details.

2.4. Chapter Summary

In this chapter, some important definitions and results about graph theory are presented, and the equilibrium states of a particular consensus algorithm are investigated. Then, two power control algorithms, which constitute the bases for the algorithms proposed in this thesis, are discussed briefly. In next chapter, we propose a new power update algorithm that stands as an alternative for the algorithm given in Section 2.3.1 in terms of feasibility.

3. A DISTRIBUTED POWER UPDATE ALGORITHM

In this chapter, we present an alternative power update algorithm (PUA-I) for the well known power control algorithm of Foschini–Miljanic [17]. In Section 2.3, it is shown that the algorithm of Foschini–Miljanic, given in (2.3), does require a predetermined target SINR value which ensures that the network is feasible. In contrast, PUA-I does not necessitate any preset SINR value, and does not face any feasibility issue. After introduction of PUA-I, its convergence and optimality analysis, along with simulation results, will be presented in the remaining sections.

3.1. Power Update Algorithm I (PUA-I)

Reconsider the downlink case of a wireless communication network model with M transmitter/receiver pairs (base station/user), where $\mathcal{I} = \{1, 2, \ldots, M\}$. Note that the communication network model can be represented by a graph denoted by $G = (V, E)$, where V represents the set of nodes (BSs, $V = \mathcal{I}$) and E denotes the set of edges (communication channels between BSs). If BSs i and j have mutual information exchange, then there exists an edge between nodes i and j in G. This implies that $j \in N_i$ (and $i \in N_j$), where N_i represents the set of BSs that have a mutual communication with BS i and $|N_i|$ denotes the cardinality of N_i. Throughout the thesis, the following is assumed to be satisfied:

Assumption 1. *The underlying graph $G = (V, E)$ of the communication network is connected.*

For a wireless communication network where the SINR of UE i is given by (2.3), the distributed power update algorithm I (PUA-I) is proposed as follows:

$$\dot{p}_i(t) = -\beta_i \Big(1 - \frac{\Gamma_{i,ref}(t)}{\Gamma_i(t)}\Big) p_i(t), \quad i \in \mathcal{I} \tag{3.1}$$

where β_i is a positive constant and $\Gamma_{i,ref}(t)$ is given by

$$\Gamma_{i,ref}(t) = \frac{1}{|N_i|} \sum_{j \in N_i} \Gamma_j(t). \tag{3.2}$$

According to the algorithm (3.1), BS i updates its transmission power by using SINR of its own UE and the reference value (3.2) which is defined as the average SINR of its close neighbors. Note that (3.1) can also be written in vector form as follows:

$$\dot{\mathbf{p}}(t) = -\mathbf{B}\mathbf{I}_{\mathbf{d}}(t)\mathbf{N}\mathbf{L}\mathbf{\Gamma}(t), \tag{3.3}$$

where $\mathbf{p}(t) = [p_1(t), p_1(t), \cdots, p_M(t)]^T$, $\mathbf{B} = \text{diag}\big[\beta_i\big]_{i=1}^{M}$, $\mathbf{\Gamma}(t) = [\Gamma_1(t), \Gamma_1(t), \cdots, \Gamma_M(t)]^T$, $\mathbf{I}_{\mathbf{d}}(t) = \text{diag}\big[I_i\big]_{i=1}^{M}$, $\mathbf{N} = \text{diag}\big[\frac{1}{|N_i|}\big]_{i=1}^{M}$, and $\mathbf{L} \in \mathbb{R}^{M \times M}$ is a symmetric positive semi-definite Laplacian matrix. As opposed to the power control algorithm presented in [17], the above algorithm does not have any feasibility issues since the use of a pre-determined target SINR value γ is not required.

3.2. Convergence Analysis of PUA-I

In this section, a detailed convergence analysis is provided for the power update algorithm given in (3.1). In order to be able to carry out convergence analysis, we need to recall the following lemmas.

Lemma 3.1. *[29] Given a differentiable function $f(t)$, if $f(t)$ is lower bounded and non-increasing ($\dot{f}(t) \leq 0$), then it converges to a limit.*

Lemma 3.2. *[29] If a differentiable function $f(t)$ converges to a limit as $t \to \infty$ and $\ddot{f}(t)$ is bounded, then, $\dot{f}(t) \to 0$ as $t \to \infty$.*

Using the properties given in Lemmas 3.1 and 3.2, the following result is presented:

Theorem 3.3. *Under Assumption 1, the proposed power update algorithm given in (3.1) converges to a fair solution $\mathbf{\Gamma}^*$, where $\Gamma_i^* = \Gamma_j^*$ holds $\forall i, j \in \mathcal{I}$.*

Proof. Consider the following function:

$$V(\mathbf{p}(t)) = \mathbf{p}^T(t)\mathbf{B}^{-1}\mathbf{p}(t) = \sum_{i=1}^{M} \frac{1}{\beta_i} p_i^2(t), \tag{3.4}$$

which is non-negative for all $t \geq 0$. Since we have $\mathbf{p}^T(t) = \mathbf{\Gamma}^T(t)\mathbf{I_d}(t)$ from (2.3), the derivative of $V(\mathbf{p}(t))$ with respect to time is expressed as

$$\begin{aligned} \dot{V}(\mathbf{p}(t)) &= \dot{\mathbf{p}}^T(t)\mathbf{B}^{-1}\mathbf{p}(t) + \mathbf{p}^T(t)\mathbf{B}^{-1}\dot{\mathbf{p}}(t), \\ &= -\mathbf{\Gamma}^T(t)\mathbf{L}\mathbf{N}\mathbf{I_d}(t)\mathbf{p}(t) - \mathbf{p}^T(t)\mathbf{I_d}(t)\mathbf{N}\mathbf{L}\mathbf{\Gamma}(t), \\ &= -2\mathbf{\Gamma}^T(t){\mathbf{I_d}}^2(t)\mathbf{N}\mathbf{L}\mathbf{\Gamma}(t), \\ &= -2\mathbf{\Gamma}^T(t)\overline{\mathbf{L}}\mathbf{\Gamma}(t), \end{aligned} \tag{3.5}$$

where $\overline{\mathbf{L}} = {\mathbf{I_d}}^2(t)\mathbf{N}\mathbf{L}$ is a non-symmetric positive semi-definite Laplacian matrix. Hence, $\dot{V}(\mathbf{p}(t)) \leq 0$ holds for all $t \geq 0$. Since $V(\mathbf{p}(t)) \geq 0$ (lower bounded) and $\dot{V}(\mathbf{p}(t))$ is non-increasing, by Lemma 3.1, $V(\mathbf{p}(t))$ converges to a limit as $t \to \infty$. This implies that $\mathbf{p}(t)$ is bounded together with $\mathbf{\Gamma}(t)$ and $\mathbf{I_d}(t)$.

Note that (3.5) can also be written as

$$\begin{aligned} \dot{V}(\mathbf{p}(t)) &= -2\sum_{i=1}^{M} p_i^2(t)\Big(1 - \frac{\Gamma_{i,ref}(t)}{\Gamma_i(t)}\Big), \\ &= -2\sum_{i=1}^{M} \frac{p_i^2(t)}{\Gamma_i(t)}\Big(\Gamma_i(t) - \Gamma_{i,ref}(t)\Big) \end{aligned} \tag{3.6}$$

whose time derivative can be expressed as

$$\ddot{V}(\mathbf{p}(t)) = -2\sum_{i=1}^{M} \frac{p_i(t)}{\Gamma_i(t)}\Big[\big(2\dot{p}_i(t)\Gamma_i(t) - \dot{\Gamma}_i(t)p_i(t)\big)\Big(1 - \frac{\Gamma_{i,ref}(t)}{\Gamma_i(t)}\Big) + p_i(t)\big(\dot{\Gamma}_i(t) - \dot{\Gamma}_{i,ref}(t)\big)\Big]. \tag{3.7}$$

Using (3.1), (3.7) can be computed as

$$\ddot{V}(\mathbf{p}(t)) = -2\sum_{i=1}^{M}\frac{p_i(t)}{\Gamma_i(t)}\Bigg[\Big(-2\beta_i p_i(t)\big(\Gamma_i(t)-\Gamma_{i,ref}(t)\big)-\dot{\Gamma}_i(t)p_i(t)\Big)\left(1-\frac{\Gamma_{i,ref}(t)}{\Gamma_i(t)}\right) + p_i(t)\Big(\dot{\Gamma}_i(t)-\frac{1}{|N_i|}\sum_{j\in N_i}\dot{\Gamma}_j(t)\Big)\Bigg], \tag{3.8}$$

and, using (2.3), $\dot{\Gamma}_i(t)$ can be calculated by

$$\begin{aligned}\dot{\Gamma}_i(t) &= \frac{d}{dt}\Big(\frac{p_i(t)}{I_i(t)}\Big) = \frac{\dot{p}_i(t)I_i(t)-p_i(t)\dot{I}_i(t)}{I_i^2(t)}\\ &= \frac{1}{I_i^2(t)}\Big[-\beta_i I_i^2(t)\big(\Gamma_i(t)-\Gamma_{i,ref}(t)\big)-p_i(t)\dot{I}_i(t)\Big]\\ &= -\beta_i\big(\Gamma_i(t)-\Gamma_{i,ref}(t)\big)-\frac{\Gamma_i(t)}{I_i(t)}\sum_{j\in\mathcal{I},j\neq i}h_{ij}\dot{p}_j(t)\\ &= -\beta_i\big(\Gamma_i(t)-\Gamma_{i,ref}(t)\big)-\frac{\Gamma_i(t)}{I_i(t)}\sum_{j\in\mathcal{I},j\neq i}h_{ij}I_j(t)\beta_j\big(\Gamma_j(t)-\Gamma_{j,ref}(t)\big).\end{aligned} \tag{3.9}$$

Since it is already shown that $I_i(t)$, $p_i(t)$, β_i, h_{ij} and $\Gamma_i(t)$ are bounded for all $t \geq 0$, which implies $\Gamma_{i,ref}(t)$ is also bounded, $\dot{\Gamma}_i(t)$ is bounded for all $t \geq 0$. Furthermore, we have $i, j \in \mathcal{I}$, where $\mathcal{I}$ has a finite number of elements. Hence, $\ddot{V}(\mathbf{p}(t))$ is bounded for all $t \geq 0$. From Lemma 3.2, we can conclude that $\dot{V}(\mathbf{p}(t)) \to 0$ as $t \to \infty$. In other words, we have

$$\lim_{t\to\infty}\mathbf{\Gamma}^T(t)\overline{\mathbf{L}}\mathbf{\Gamma}(t) = 0 \tag{3.10}$$

which implies $\overline{\mathbf{L}}\mathbf{\Gamma}(t) = 0$ when $t \to \infty$. Since the underlying graph of the communication network is assumed to be connected (Assumption 1), the Laplacian matrix $\mathbf{L}$ has a simple eigenvalue at zero [26]. Since $\beta_i > 0$, $I_i(t) > 0$ holds for all $i \in \mathcal{I}$ and for all $t \geq 0$, the non-symmetric Laplacian matrix $\overline{\mathbf{L}}$ has also a simple eigenvalue at zero, and its non-zero eigenvalues have strictly positive real parts [30]. Hence, $\dot{V}(\mathbf{p}(t)) = 0$ implies $\dot{\mathbf{p}}(t) = 0$ and we can conclude from (3.3) and (3.10) that $\Gamma_i^* = \Gamma_j^*$ holds for all $i, j \in \mathcal{I}$.

□

Remark 1. *The proposed power update algorithm (PUA-I) given in (3.1) not only overcomes the problem of an infeasible choice of pre-determined target SINR value γ, but also provides fairness among UEs in the network by achieving the same SINR level for each user in the network.*

3.3. Optimality Analysis

In this section, optimality analysis of the PUA-I which is given in (3.1) is carried out. For the theoretical analysis, the non–negativity of SINR and power vectors are first discussed in the following Lemma and its corollary.

Lemma 3.4. *Starting with any positive initial power assignment vector $\mathbf{p}(t_0) > 0$, transmission powers of all base stations always remain non–negative, i.e., $\mathbf{p}(t) \geq 0, \forall t \geq t_0$.*

Proof. For BS i to have a negative transmission power, there should exist an instant t_1 such that $p_i(t_1) = 0$ and $\dot{p}_i(t_1) < 0$. By using (2.3) and (3.2), (3.1) can be rewritten as

$$\begin{aligned} \dot{p}_i(t_1) &= -\beta_i\Big(p_i(t_1) - \Gamma_{i,ref}(t_1)I_i(t_1)\Big) \\ &= \beta_i I_i(t_1)\frac{1}{|N_i|}\sum_{j\in N_i}\Gamma_j(t_1), \end{aligned} \tag{3.11}$$

which is always non–negative and becomes zero only when $p_i(t_1) = 0, \forall i \in \mathcal{I}$. Therefore, $p_i(t_1) = 0$ contradicts with $\dot{p}_i(t_1) < 0$. □

As a natural extention of Lemma 3.4, starting with an arbitrary initial power assignment vector $\mathbf{p}(t_0) > 0$, SINR values always remain non–negative, i.e., $\Gamma_i(t) \geq 0$ for all $t \geq t_0$.

With the given Lemma 3.4, the following two lemmas, where the second one is also known as Perron theorem, are also required for the optimality analysis:

Lemma 3.5. *(see 8.5.2 in [31]) If matrix $\mathbf{A} \in \mathbb{R}^{m\times m}$ is non–negative, then $\mathbf{A}$ is primitive if and only if $\mathbf{A}^n > 0$ for some $n \geq 1$.*

Lemma 3.6. *(Perron Theorem, [32, 33]) Let $r(\mathbf{A})$ denote the spectral radius of matrix $\mathbf{A} \in \mathbb{R}^{m\times m}$ (i.e., $r(\mathbf{A}) = \max\{|\lambda_1|,\ldots,|\lambda_m|\}$). For a primitive non–negative square matrix $\mathbf{A}$, there exists a positive real eigenvalue $\lambda = r(\mathbf{A})$ with algebraic multiplicity 1, where the modulus of the other eigenvalues are strictly less than $r(\mathbf{A})$. The corresponding right eigenvector of λ, also known as the Perron eigenvector, is positive and it is the only non–negative eigenvector of $\mathbf{A}$.*

Using Theorem 3.3, and Lemmas 3.5 and 3.6, we state the following result for the noise free systems:

Theorem 3.7. *When the system is assumed to be noise free (i.e., $\eta_i = 0, \forall i \in \mathcal{I}$), the PUA-I, given in (3.1), converges to a unique fair solution $\gamma^* = \frac{1}{r(\mathbf{H})}$, where $r(\mathbf{H})$ is the spectral radius of $\mathbf{H}$ which is defined as an M-dimensional square matrix with zero diagonal and positive $h_{ij} = \frac{g_{ij}}{g_{ii}}$ values on the off-diagonals.*

Proof. As stated in Theorem 3.3, the SINR values of the network converge to a fair solution (i.e., $\Gamma_i = \gamma^*,\ \forall i \in \mathcal{I}$). In a noise free system, once the consensus is reached, (2.3) can be written as

$$\Gamma_i = \frac{p_i^*}{\sum\limits_{j\in\mathcal{I}, j\neq i} h_{ij}p_j^*} = \gamma^*, \forall i \in \mathcal{I}, \tag{3.12}$$

which, in vector form, becomes

$$\mathbf{H}\mathbf{p}^* = \tfrac{1}{\gamma^*}\mathbf{p}^*. \tag{3.13}$$

Since $\mathbf{H}^c > 0$ for all $c \geq 2$, by Theorem 3.5, the non-negative $\mathbf{H}$ matrix is found to be primitive. As stated in Lemma 3.4, power vector $\mathbf{p}(t)$ always remains non–negative. Then, by Theorem 3.6, it can be concluded that the only feasible solution for (3.13) is $\gamma^* = \frac{1}{r(\mathbf{H})}$ and $\mathbf{p}^*$ equals to the corresponding eigenvector of $r(\mathbf{H})$. □

Remark 2. *Since* $\mathbf{H}$ *matrix does not contain any variable related with initial transmission power values, the final SINR value that every UE converges (*$\gamma^* = \frac{1}{r(\mathbf{H})}$*), is the same for all positive initial power assignment vectors.*

In order to analyse the optimality of the system, in which thermal noise is not neglected (i.e., $\boldsymbol{\eta} \geq 0 \ \ (\boldsymbol{\eta} \neq 0)$), we need to recall the following theorem:

Lemma 3.8. *[34] Let* $\mathbf{A} \in \mathbb{R}^{m\times m}$ *be an irreducible non–negative matrix. Then,* $\mathbf{A}$ *has a simple positive eigenvalue* λ *equal to* $r(\mathbf{A})$*, and positive eigenvectors* α *and* $\tilde{\alpha}$ *associated with* λ*, such that* $\mathbf{A}\alpha = \lambda\alpha$ *and* $\mathbf{A}^T\tilde{\alpha} = \lambda\tilde{\alpha}$*. Given the following valid vector norms* $\|\cdot\|_{(p)}$

$$\|v\|_{(p)} = \begin{cases} \left[\sum_{i=1}^{n} \tilde{\alpha}_i \alpha_i \left(\frac{|v_i|}{\alpha_i}\right)^p\right]^{1/p}, & for\ 1 \leq p < \infty, \\ \max_{i=1,\ldots,m} \frac{|v_i|}{\alpha_i}, & for\ p = \infty, \end{cases} \tag{3.14}$$

weighted Hölder norms of the irreducible non–negative matrix $\mathbf{A} \in \mathbb{R}^{m\times m}$ *can be defined as* $\|\mathbf{A}\|_{(p)} = \sup_{\|v\|=1} \|\mathbf{A}v\|_{(p)}$*. Then,* $\|\mathbf{A}\|_{(p)} = r(\mathbf{A})$ *holds for all* $1 \leq p \leq \infty$*.*

When the thermal noise in the system is not neglected (i.e., $\boldsymbol{\eta} \geq 0 \ \ (\boldsymbol{\eta} \neq 0)$), the maximum achievable solution can be found by the following theorem:

Theorem 3.9. *For a network modeled by (2.3), given any* ε *such that* $0 < \varepsilon < \frac{1}{r(\mathbf{H})}$*, there exists a finite positive solution* $\mathbf{p}^*$ *that satisfies* $\Gamma_i = \frac{1}{r(\mathbf{H})} - \varepsilon$*, for all* $i \in \mathcal{I}$*.*

Proof. When all UEs have the same SINR value (i.e., $\Gamma_i = \gamma^*, \ \forall i \in \mathcal{I}$), (2.3) can be written as

$$\Gamma_i = \frac{p_i^*}{\sum_{j\in\mathcal{I}, j\neq i} h_{ij}p_j^* + \eta_i} = \gamma^*, \forall i \in \mathcal{I}, \tag{3.15}$$

which can be represented in vector form as follows:

$$\left(\tfrac{1}{\gamma^*}\mathbf{I} - \mathbf{H}\right)\mathbf{p}^* = \boldsymbol{\eta}. \tag{3.16}$$

Here, $\mathbf{I}$ is the $M \times M$ identity matrix, $\mathbf{H}$ is an M-dimensional square matrix with zero diagonal and positive $h_{ij} = \frac{g_{ij}}{g_{ii}}$ values on the off-diagonals, $\boldsymbol{\eta}$ denotes an M-dimensional vector containing η_i values which are non–negative. In order to find a feasible $\mathbf{p}^*$ (non–negative power vector) solution to (3.16) for all possible non–negative $\boldsymbol{\eta}$ vectors, $\left(\frac{1}{\gamma^*}\mathbf{I} - \mathbf{H}\right)$ should be a monotone matrix. Since this matrix has non–positive off-diagonal entries, being monotone equivalently means being an M–matrix [27]. Thus, we can conclude that for (3.16) to have a feasible solution, γ^* can not exceed an upper limit (i.e., $\gamma^* \leq \frac{1}{r(\mathbf{H})}$). Since $\gamma^* = \frac{1}{r(\mathbf{H})}$ makes $\left(\frac{1}{\gamma^*}\mathbf{I} - \mathbf{H}\right)$ singular, maximum achievable SINR value is defined by a strict inequality.

Given ε, let $\alpha = \varepsilon r(\mathbf{H})$. Then, γ^* becomes $\gamma^* = \frac{(1-\alpha)}{r(\mathbf{H})}$, and the solution $\mathbf{p}^*$ for (3.16) can be written as

$$\mathbf{p}^* = \left(\mathbf{I} - \frac{(1-\alpha)}{r(\mathbf{H})}\mathbf{H}\right)^{-1} \frac{(1-\alpha)}{r(\mathbf{H})}\boldsymbol{\eta}. \tag{3.17}$$

Note that $0 < \alpha < 1$. Since $(1-\alpha) < 1$, the modulus of the largest eigenvalue of $\frac{(1-\alpha)}{r(\mathbf{H})}\mathbf{H}$ is found to be less than 1, and we have the following equation [35]:

$$\left(\mathbf{I} - \frac{(1-\alpha)}{r(\mathbf{H})}\mathbf{H}\right)^{-1} = \mathbf{I} + \sum_{i=1}^{\infty}\left(\frac{(1-\alpha)}{r(\mathbf{H})}\mathbf{H}\right)^{i}. \tag{3.18}$$

By using (3.18), we can rewrite (3.17) as

$$\begin{aligned}
\mathbf{p}^* &= \frac{(1-\alpha)}{r(\mathbf{H})}\boldsymbol{\eta} + \left[\sum_{i=1}^{\infty}\left(\frac{(1-\alpha)}{r(\mathbf{H})}\mathbf{H}\right)^{i}\right]\frac{(1-\alpha)}{r(\mathbf{H})}\boldsymbol{\eta} \\
&= \frac{(1-\alpha)}{r(\mathbf{H})}\boldsymbol{\eta} + \left(\frac{(1-\alpha)}{r(\mathbf{H})}\right)^{2}\mathbf{H}\boldsymbol{\eta} + \left(\frac{(1-\alpha)}{r(\mathbf{H})}\right)^{3}\mathbf{H}^2\boldsymbol{\eta} + \ldots \\
&= \frac{(1-\alpha)}{r(\mathbf{H})}\boldsymbol{\eta} + \frac{(1-\alpha)}{r(\mathbf{H})}\mathbf{H}\left[\frac{(1-\alpha)}{r(\mathbf{H})}\boldsymbol{\eta} + \left(\frac{(1-\alpha)}{r(\mathbf{H})}\right)^{2}\mathbf{H}\boldsymbol{\eta} + \left(\frac{(1-\alpha)}{r(\mathbf{H})}\right)^{3}\mathbf{H}^2\boldsymbol{\eta} + \ldots\right] \\
&= \frac{(1-\alpha)}{r(\mathbf{H})}\boldsymbol{\eta} + \frac{(1-\alpha)}{r(\mathbf{H})}\mathbf{H}\mathbf{p}^*,
\end{aligned} \tag{3.19}$$

Since $\mathbf{H}$ is an M-dimensional square matrix with zero diagonal and positive entries on off-diagonals, it satisfies $(\mathbf{I}+\mathbf{H})^{M-1} > 0$ and found to be an irreducible non–negative matrix (Lemma 8.4.1. in [31]). By Perron–Frobenius (Theorem 3.9 in [32]), $\mathbf{H}$ has a simple eigen-

value which equals to $r(\mathbf{H})$, and the corresponding right eigenvector of $r(\mathbf{H})$, denoted as v, is the only strictly positive eigenvector of $\mathbf{H}$. By using the weighted Hölder norm described in Lemma 3.8, the infinity norm of $\mathbf{p}^*$ can be written as

$$\begin{aligned}
\|\mathbf{p}^*\|_\infty &= \left\| \frac{(1-\alpha)}{r(\mathbf{H})}\boldsymbol{\eta} + \frac{(1-\alpha)}{r(\mathbf{H})}\mathbf{H}\mathbf{p}^* \right\|_\infty \\
&= \frac{(1-\alpha)}{r(\mathbf{H})} \|\boldsymbol{\eta} + \mathbf{H}\mathbf{p}^*\|_\infty \\
&\leq \frac{(1-\alpha)}{r(\mathbf{H})} \|\boldsymbol{\eta}\|_\infty + \frac{(1-\alpha)}{r(\mathbf{H})} \|\mathbf{H}\mathbf{p}^*\|_\infty \\
&\leq \frac{(1-\alpha)}{r(\mathbf{H})} \|\boldsymbol{\eta}\|_\infty + \frac{(1-\alpha)}{r(\mathbf{H})} \|\mathbf{H}\|_\infty \|\mathbf{p}^*\|_\infty \\
&= \frac{(1-\alpha)}{r(\mathbf{H})} \|\boldsymbol{\eta}\|_\infty + (1-\alpha) \|\mathbf{p}^*\|_\infty . \qquad (3.20)
\end{aligned}$$

Then, by using (3.19) and (3.20), lower and upper bounds for $\|\mathbf{p}^*\|_\infty$ can be expressed as

$$\frac{(1-\alpha)}{r(\mathbf{H})} \|\boldsymbol{\eta}\|_\infty \;<\; \|\mathbf{p}^*\|_\infty \;\leq\; \frac{1}{\alpha}\frac{(1-\alpha)}{r(\mathbf{H})} \|\boldsymbol{\eta}\|_\infty . \qquad (3.21)$$

Thus, using the vector norm definition given in (3.14), it can be concluded that $\mathbf{p}^*$ is finite for all $0 < \alpha < 1$. □

3.4. Simulation Results of PUA-I

In this section, numerical analysis for PUA-I is presented. Simulation topology which is given in Figure 3.1 consists of 8 transmitter/receiver pairs. Simulations are carried out for the downlink case and each BS (transmitter) is assumed to be causing interference on the UE of every other BS. Dashed lines represent the communication links, on which the required information is carried between the BSs. The collection of all dashed lines represents the underlying graph which is connected for this network. Simulations of the algorithm are done by its discrete time implementation. Using Euler's approximation, PUA-I can be discretized as

$$p_i[k+1] = p_i[k] - T_s\beta_i\Big(1 - \frac{\Gamma_{i,ref}[k]}{\Gamma_i[k]}\Big)p_i[k], \quad i \in \mathcal{I}, \qquad (3.22)$$

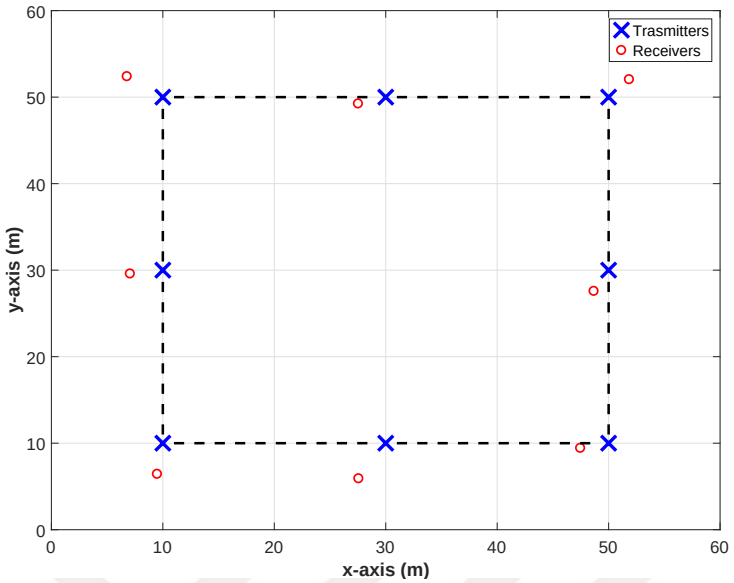

Figure 3.1. PUA-I simulation topology with edges.

where $T_s = 10ms$ denotes the sampling period, and update constant β_i is chosen as 8 for all BSs. All BSs start executing the algorithm with randomly chosen initial transmission powers less than 33 dBm (2 Watt), where the thermal noise power is taken the same as -80 dBm (10^{-11} Watt) on all UEs. The channel gains are calculated by $g_{i,j} = \chi^{(i)} d_{i,j}^{-\alpha}$, where $d_{i,j}$ is the physical distance between UE i and interfering BS j. $\chi^{(i)}$ value is generated randomly, and taken as [1.1331 1.2070 1.5913 1.3960 1.5561 1.5399 1.5723 1.1704] for each BS/UE pair. Path loss exponent is taken as $\alpha = 3$.

Simulation results are given in Figure 3.2. In the first $5s$, UEs stand still in their first locations as given in Figure 3.1. As theoretically expected, SINR of all UEs converges to a common value in this period. Then, from $t = 5s$ to $t = 10s$, UEs are moved randomly with a velocity of $v = 1m/s$. Each of these motions is realised as a Brownian motion with constant step size (i.e. $\Delta d = v/T_s$) and random direction in each iteration. For this time interval, SINR values are constantly changing due to the motions of the UEs. After $t = 10s$, UEs stop moving and are seen to be converging to a common SINR again. In summary, by this simulation result, we see that the PUA-I can be used in the networks with dynamic topology.

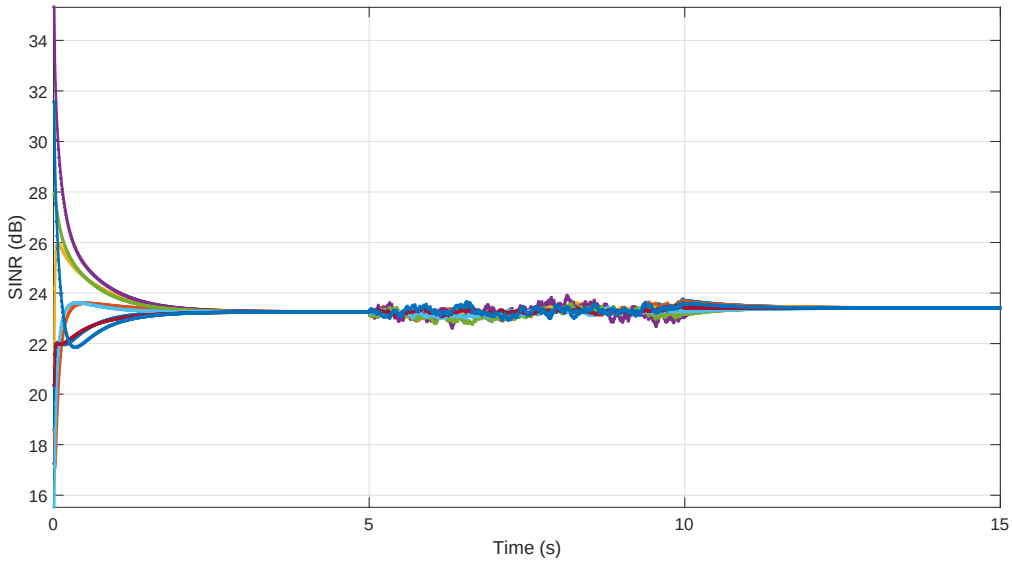

Figure 3.2. Simulation results of PUA-I with mobility.

3.5. Chapter Summary

In this chapter, a distributed power update algorithm (PUA-I) is proposed as an alternative for the well known algorithm of Foschini-Miljanic. It is analytically shown that the PUA-I is stable for connected networks and it converges to the optimal fair solution. These results are also illustrated by simulations. In the next chapter, we extend this algorithm, and the algorithm given in Section 2.3.2, for the OFDMA femtocell networks where BSs can have more than one UE.

4. DISTRIBUTED POWER UPDATE ALGORITHMS FOR OFDMA FEMTOCELL NETWORKS

In the network model considered for PUA-I (proposed in (3.1)) and PCA (given in 2.7), all BSs are assumed to serve a single UE on the same frequency channel. However, in real life OFDMA femtocell networks, BSs are designed to serve more than a single UE, and the available spectrum is divided into multiple subchannels. Also by its nature, a joint power/frequency allocation problem should include multiple number of subchannels. In order to make the given power control algorithms (PUA-I and PCA) more realistic, and more usable in joint resource allocation problems, they need to be modified in such a way that they ensure the global fairness among all of their users.

In this chapter, we propose two new power update algorithms (PUA-II and PUA-III) which are respectively the multi–user extensions of PUA-I and the PCA [18]. The modifications are made by expanding the corresponding graph of inter–base station communication network in a way that each node splits into virtual nodes by the number of its active subchannels. As a result, each BS updates its transmission power levels by using information coming from its neighboring BSs and its own users. Expansion of the corresponding graphs can be visualised better in Figure 4.1. Figure 4.1(a) shows the underlying graph of an example network consisting of 3 transmitter/receiver pairs. Here, the small and dashed circles respectively represent the BSs and their coverage areas, where the straight lines represent the communication links between neighboring BSs. When each BS has 4 active subchannel/UE pairs, and PUA-II (or PUA-III) is used, the underlying communication graph expands as shown in Figure 4.1(b).

In the rest of this chapter, first, the system model will be introduced. Then, the proposed algorithms (PUA-II and PUA-III) will be presented. Next, before concluding the chapter, the simulation results will be given.

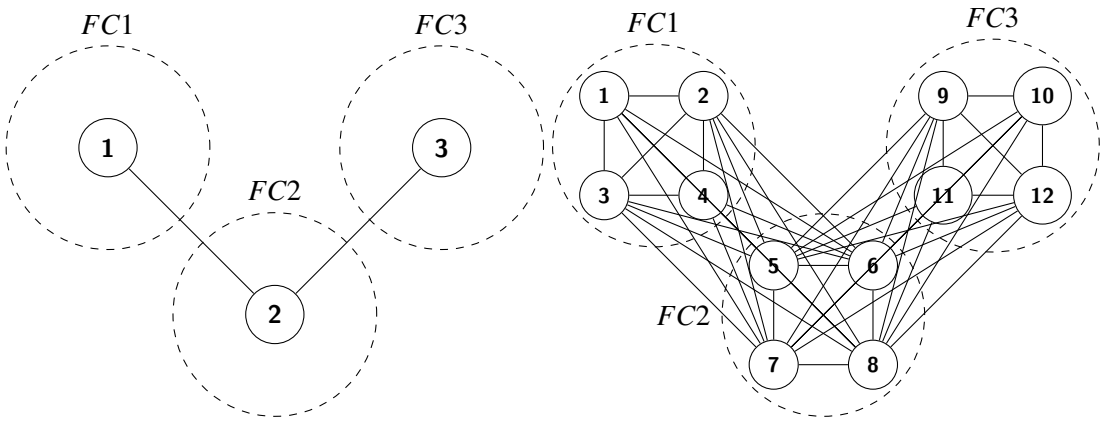

(a) Underlying graph for PUA-I and PCA (b) The expanded graph for PUA-II and PUA-III

Figure 4.1. Expansion of the underlying graph for a network with 3 BSs

4.1. System Model for OFDMA Femtocell Networks

System model considers the downlink case of a two–tier femtocell network. The first tier consists of a single MBS and its UEs. Within the coverage area of the MBS, there exist M_f FBSs each may have different number of UEs. These FBSs and FUEs constitute the second tier of the network. The set of all BSs is denoted as $\mathcal{M} = \{0, 1, \ldots, M_f\}$ where 0 corresponds to the MBS and others to FBSs. $\mathcal{K}_m$ and K_m respectively denote the set and number of UEs served by BS m, where $m \in \mathcal{M}$. The spectrum, which is divided into S OFDMA frequency subchannels, is available for both MBS and FBSs. The set of available subchannels is given by $\mathcal{S} = \{1, 2, \ldots, S\}$, where a subchannel can be assigned at most to one UE within a cell. Therefore, intra–cell interference is eliminated by the orthogonality of subchannels.

Connection status between BS m and UE k on subchannel s, $k \in \mathcal{K}_m$, is denoted by $\rho^s_{m,k}$. If BS m provide service to UE k on subchannel s, $\rho^s_{m,k} = 1$. Otherwise, $\rho^s_{m,k} = 0$. In the model, it is possible for BS m to have more (or less) UEs than the number of available subchannels (i.e. $K_m \neq S$). Let the subchannels that are assigned to a UE in a given cell be called "active", then $\mathcal{U}_m$ and U_m respectively denote the set of active subchannels of cell m and that set's cardinality. When we turn the set $\mathcal{U}_m$ into a vector by sorting elements in ascending order, we obtain the u_m vector which has the information of active subchannels

in BS m. For instance, $\mathcal{U}_2 = \{1,4,7\}$ and $u_2 = [1,4,7]^T$ correspond to the set and vector of subchannels that are in use by BS 2, respectively. Then, we can define $U_m = |u_m|$ as follows:

$$U_m = |\mathcal{U}_m| = min(S, K_m). \tag{4.1}$$

If we patch all the u_m vectors, starting from BS 1 to BS M_f, we get vector u which shows all the active subchannels in the femtocell network:

$$u = [u_1^T, \ldots, u_{M_f}^T]^T. \tag{4.2}$$

Then, the length of vector u, which is equal to total number of all active subchannels of the entire femtocell network, can be calculated as

$$U = \sum_{i \in \mathcal{M} \setminus \{0\}} min(S, K_i). \tag{4.3}$$

At time instant t, transmission power of BS m on subchannels s is denoted by $p_m^s(t)$. Then, we can define a vector $\widetilde{p}_m(t)$, which has the identical order as u_m, such that it contains power values assigned to active subchannels of BS m (e.g., for $u_2 = [1,4,7]^T$, $\widetilde{p}_2(t) = [\widetilde{p}_2^1(t), \widetilde{p}_2^4(t), \widetilde{p}_2^7(t)]^T$). Then, the following vector, which has the length U, contains transmission powers on all the active subchannels used by FBSs of the entire network:

$$\widetilde{\mathbf{p}}(t) = [\widetilde{p}_1^T(t), \widetilde{p}_2^T(t), \ldots, \widetilde{p}_{M_f}^T(t)]^T. \tag{4.4}$$

For fixed channel assignment, SINR of the downlink signal from BS m to UE k on subchannel s, where $k \in \mathcal{K}_m$, can be defined as

$$\Gamma_{m,k}^s(t) = \rho_{m,k}^s \frac{p_m^s(t)}{\sum\limits_{j \in \mathcal{M} \setminus m} h_{(m,j),k}^s p_j^s(t) \; + \; \eta_{m,k}^s} = \rho_{m,k}^s \frac{p_m^s(t)}{I_{m,k}^s(t)} \quad , \quad k \in \mathcal{K}_m, \tag{4.5}$$

where $h^s_{(m,j),k} = \frac{g^s_{j,k}}{g^s_{m,k}}$ and $\eta^s_{m,k} = \frac{\sigma^s_k}{g^s_{m,k}}$. $\rho^s_{m,k}$ multiplier makes SINR value 0 when the BS m does not serve UE k on the subchannel s, where $k \in \mathcal{K}_m$. Also, $g^s_{m,k}$ is the downlink channel gain between UE k and BS m on subchannel s, where $\sigma^s_k \geq 0$ denotes the power of thermal noise received by UE k on subchannel s.

A base station can assign an OFDMA subchannel to at most one UE. Therefore, for the fixed m and k values, there will be at most one non–zero $\Gamma^s_{m,k}(t)$ variable for all $s \in \mathcal{S}$. That means, without loss of generality, we can eliminate the k term in $\Gamma^s_{m,k}(t)$, and let $\Gamma^s_m(t)$ denote the SINR on subchannel s in cell m, regardless of which UE is using that subchannel. Then, the average SINR of the users served by BS m can be calculated as

$$\Gamma_{m,ave}(t) = \frac{\sum\limits_{i \in \mathcal{U}_m} \Gamma^i_m(t)}{U_m}. \tag{4.6}$$

4.2. Power Update Algorithm II (PUA-II)

In this section, a consensus-based power update algorithm (PUA-II), whose objective is to provide fairness among all femtocell users, is presented. Starting with random, but feasible, $\widetilde{\mathbf{p}}(0)$ vector, where subchannel assignment is assumed to be fixed, each femtocell m in the network uses the following power update algorithm:

$$\dot{p}^s_m(t) = -\beta^s_m \left[1 - \frac{\Gamma^s_{m,ref}(t)}{\Gamma^s_m(t)}\right] p^s_m(t), \tag{4.7}$$

where

$$\Gamma^s_{m,ref}(t) = \frac{1}{U_m - 1 + \sum\limits_{j \in N_m} U_j} \left[\sum_{j \in N_m} U_j \Gamma_{j,ave}(t) + \sum_{i \in \mathcal{U}_m \setminus s} \Gamma^i_m(t)\right], \quad s \in \mathcal{U}_m. \tag{4.8}$$

Here, β^s_m is a positive constant that determines the update speed of the transmission power of BS m, on subchannel s. N_m denotes the set of close neighbours of BS m. In order to execute the PUA-II given in (4.7), BS m requires 2 external information from its neighbours:

Average SINR values on their actively used subchannels ($\Gamma_{j,ave}(t),\ \forall j \in N_m$) and the number of these actively used subchannels ($U_j,\ \forall j \in N_m$). The other required information (i.e. U_m and $\Gamma_m^i,\ i \in \mathcal{S} \setminus s$) is already known by the BS m. It is also assumed that BS m does not execute this algorithm on power update of subchannel s if there is no user assigned to that subchannel. Instead, power on that subchannel is kept zero in order to prevent additional interferences on other cells. It should also be noted that BS m needs to execute this algorithm in a parallel fashion for each of its active subchannels.

In vector notation, (4.7) can be rewritten as

$$\dot{\widetilde{\mathbf{p}}}(t) = -\widetilde{\mathbf{B}}\widetilde{\mathbf{I}}_{\mathbf{d}}(t)\widetilde{\mathbf{N}}\widetilde{\mathbf{L}}\widetilde{\mathbf{\Gamma}}(t), \tag{4.9}$$

where $\widetilde{\mathbf{\Gamma}}(t)$ is the vector that contains the SINR values of active subchannels of entire femtocell network. It has the same length (U) and identical order as $\widetilde{\mathbf{p}}(t)$ given in (4.4). $\widetilde{\mathbf{B}}$ and $\widetilde{\mathbf{I}}_{\mathbf{d}}(t)$ are $U \times U$ diagonal matrices with respectively $\beta_m^s > 0$ and $\widetilde{I}_m^s = \widetilde{p}_m^s/\widetilde{\Gamma}_m^s > 0$ values on the diagonals. $\widetilde{\mathbf{N}}$ is also a diagonal matrix with positive entries. Finally, $\widetilde{\mathbf{L}} \in \mathbb{R}^{U \times U}$ is the symmetric positive semi–definite Laplacian matrix.

Having described the overall system dynamics, the following result reveals the convergence properties of PUA-II given in (4.7).

Theorem 4.1. *Under Assumption 1, the proposed power update algorithm (PUA-II) given in (4.7) converges to a fair solution $\widetilde{\mathbf{\Gamma}}^*$, where $\widetilde{\Gamma}_i^{s^*} = \widetilde{\Gamma}_j^{\bar{s}^*}$ holds for all $s \in \mathcal{U}_i$, $\bar{s} \in \mathcal{U}_j$, and $i, j \in \mathcal{M} \setminus \{0\}$.*

Proof. Since the overall system dynamics given in (4.9) are exactly the same as the ones given in (3.3), the proof directly follows from Theorem 3.3. □

Remark 3. *The proposed power update algorithm given in (4.7) does not require high computational power, and the communication cost is minimized by keeping all the communication exchange in the network minimal.*

4.3. Power Update Algorithm III (PUA-III)

In this section, we present a new distributed power update algorithm (PUA-III) which is the multiple subchannel/UE extension of the power control algorithm (PCA) given in (2.7). A detailed study on PUA-III is also presented in [36]. PUA-III can described as follows:

$$\dot{p}_m^s(t) = -\beta_m^s \frac{\Gamma_m^s(t)}{p_m^s(t)} \left[f_m^s(t)\Gamma_m^s(t) - \sum_{j \in N_m} f_{m,j}(t)\Gamma_{j,ave}(t) - \sum_{i \in \mathcal{S} \setminus s} \tilde{f}_m^i(t)\Gamma_m^i(t) \right], s \in \mathcal{U}_m. \tag{4.10}$$

Here, the term β_m^s is a positive value and it determines the update speed of the transmission power of BS m, on subchannel s. Please notice that a high update constant β_m^s may help us to reach consensus more quickly, but it may also cause overshoots in transmission powers. N_m is the set of neighboring cells of BS m. $\Gamma_{j,ave}(t)$ term, where $j \in N_m$, denotes the average SINR value of the UEs of BS j, and it is given by (4.6). The $f_{m,j}(t)$ terms stand for the inter–cell connection weights between the base stations. $\tilde{f}_m^i(t)$ terms are the intra–cell connection weights between the same cell's subchannels which are considered as imaginary nodes of the underlying graph. $f_m^s(t)$ is the weight that determines the importance of $\Gamma_m^s(t)$ while updating the transmission power of BS m on subchannel s. Some possible choices will be shown in Section 4.3.1.

By using (4.10), BS m updates its transmission power on subchannel s in the following way: BS m collects information of the average SINR values, which is denoted as $\Gamma_{j,ave}(t)$ where $j \in N_m$, coming from its neighboring BSs. By the first summation sign inside the bracket, BS m adds up these average SINR values after multiplying them by inter–cell connection weights $f_{m,j}$. Then, by the second summation sign, it adds up the SINR values of its own subchannels other than s, after multiplying them by intra–cell connection weights $\tilde{f}_m^i(t)$. These SINR values are represented by $\Gamma_m^i(t)$, where $i \in \mathcal{S} \setminus s$. Finally, these two summation results are compared with $\Gamma_m^s(t)$ to decide the change in the transmission power $p_m^s(t)$.

For better understanding of the PUA-III, it should be stressed that BS m does not update its transmission power on s if there is no user assigned to that subchannel (i.e., $\rho_{m,k}^s = 0,\ \forall k \in \mathcal{K}_m$).

4.3.1. An Example Choice for Weights

The intra–cell connection weights $\tilde{f}_m^s(t)$ are predefined by the corresponding BS in cell m. They represent the status whether the subchannel s is in use or not. An example choice, where BS m gives equal priority to all of its UEs, can be as follows:

$$\tilde{f}_m^s(t) = \begin{cases} 1, & s \in \mathcal{U}_m, \\ 0, & \text{otherwise.} \end{cases}, \quad s \in \mathcal{S},\ m \in \mathcal{M} \setminus \{0\}. \tag{4.11}$$

Here, if the subchannel s is assigned to any UE by BS m, that subchannel's intra–cell weight is taken as 1, otherwise it is 0. It should be noted that instead of 1, we could also pick any other positive number, which would change the weighted priority of the subchannel s among the other subchannels, in the cell m.

The term $f_{m,j}(t)$ denotes the weight of the inter–cell information link from BS j to BS m. An example selection of these parameters can be done by cell j according to the number subchannels that are in use. These choices are mathematically described as

$$f_{m,j}(t) = U_j, \quad j \in N_m, \tag{4.12}$$

where U_j is defined in (4.1). According to this choice of parameters, each BS sends the total number of its active subchannel to the neighboring BSs. It is important to see that all the UEs in the network have the same priority when the intra–cell and inter–cell weights are chosen as (4.11) and (4.12). The relative priorities between the UEs could be changed by another choice of weight parameters.

For connection matrix $\mathbf{L}$, which is defined later in Section 4.3.2, to be a Laplacian, it should have zero row sums [22]. This can be satisfied by choosing the $f_m^s(t)$ weights as follows:

$$f_m^s(t) = \sum_{i \in \mathcal{S} \setminus s} \tilde{f}_m^i(t) + \sum_{j \in N_m} f_{m,j}(t). \tag{4.13}$$

4.3.2. Convergence Analysis of PUA-III

For the sake of simplicity, convergence analysis of the proposed algorithm (PUA-III) is carried out by fixing the weights as given in (4.11), (4.12), and (4.13). By these weight choices, PUA-III given in (4.10) becomes:

$$\dot{p}_m^s(t) = -\beta_m^s \frac{\Gamma_m^s(t)}{p_m^s(t)} \left[\left(U_m - 1 + \sum_{j \in N_m} U_j \right) \Gamma_m^s(t) - \sum_{j \in N_m} \sum_{i \in \mathcal{U}_j} \Gamma_j^i(t) - \sum_{i \in \mathcal{U}_m \setminus s} \Gamma_m^i(t) \right], s \in \mathcal{U}_m. \tag{4.14}$$

For later use, (4.14) can alternatively be simplified as

$$\dot{p}_m^s(t) = -\beta_m^s \frac{{\Gamma_m^s}^2(t)}{p_m^s(t)} Z_m \left[1 - \frac{\Gamma_{m,ref}^s(t)}{\Gamma_m^s(t)} \right], s \in \mathcal{U}_m, \tag{4.15}$$

where Z_m is defined as

$$Z_m = U_m - 1 + \sum_{j \in N_m} U_j, \tag{4.16}$$

and $\Gamma_{m,ref}^s(t)$ is given by

$$\Gamma_{m,ref}^s(t) = \frac{\sum_{j \in N_m} U_j \Gamma_{j,ave}(t) + \sum_{i \in \mathcal{U}_m \setminus s} \Gamma_m^i(t)}{Z_m}, \quad s \in \mathcal{U}_m. \tag{4.17}$$

In vector notation, (4.14) corresponds to

$$\dot{\widetilde{\mathbf{p}}}(t) = -\widetilde{\mathbf{B}} \widetilde{\mathbf{I}}_{\mathbf{d}}^{-1}(t) \widetilde{\mathbf{L}} \widetilde{\mathbf{\Gamma}}(t), \tag{4.18}$$

where $\widetilde{\mathbf{\Gamma}}(t)$ is the vector that contains the SINR values of active subchannels of entire femtocell network. The length of $\widetilde{\mathbf{\Gamma}}(t)$ is U, and its has identical order as $\widetilde{\mathbf{p}}(t)$ defined in (4.4). $\widetilde{\mathbf{B}}$ and $\widetilde{\mathbf{I}}_{\mathbf{d}}(t)$ are $U \times U$ diagonal matrices with respectively $\beta_m^s > 0$ and $\widetilde{I}_m^s = \widetilde{p}_m^s / \widetilde{\Gamma}_m^s > 0$ values on diagonals. Lastly, $\widetilde{\mathbf{L}} \in \mathbb{R}^{U \times U}$ is the symmetric positive semi–definite Laplacian matrix.

For the specific choice of weights defined in (4.11), (4.12), and (4.13), we state the following theorem for the convergence properties of PUA-III.

Theorem 4.2. *When Assumption 1 is satisfied and the weights are chosen as described in (4.11), (4.12), and (4.13), PUA-III given in (4.10) converges to a fair solution* $\widetilde{\mathbf{\Gamma}}^*$*, where* $\widetilde{\Gamma}_i^{s^*} = \widetilde{\Gamma}_j^{\bar{s}^*}$ *holds for all* $s \in \mathcal{U}_i$*,* $\bar{s} \in \mathcal{U}_j$*, and* $i, j \in \mathcal{M} \setminus \{0\}$.

Proof. Consider the following function:

$$V(\widetilde{\mathbf{p}}(t)) = \widetilde{\mathbf{p}}^T(t)\widetilde{\mathbf{B}}^{-1}\widetilde{\mathbf{p}}(t) = \sum_{i \in \mathcal{M}\setminus\{0\}} \sum_{s \in \mathcal{U}_i} \frac{1}{\beta_i^s} p_i^{s2}(t), \tag{4.19}$$

which is defined as sum of squares, meaning that it is non-negative for all $t \geq 0$. For fixed subchannel assignment vector, from (4.5), we have $\widetilde{\mathbf{p}}(t) = \widetilde{\mathbf{I}_\mathbf{d}}(t)\widetilde{\mathbf{\Gamma}}^T(t)$. Then, the derivative of $V(\widetilde{\mathbf{p}}(t))$ with respect to time is expressed as

$$\begin{aligned} \dot{V}(\widetilde{\mathbf{p}}(t)) &= \dot{\widetilde{\mathbf{p}}}^T(t)\widetilde{\mathbf{B}}^{-1}\widetilde{\mathbf{p}}(t) + \widetilde{\mathbf{p}}^T(t)\dot{\widetilde{\mathbf{B}}}^{-1}\widetilde{\mathbf{p}}(t), \\ &= -\widetilde{\mathbf{\Gamma}}^T(t)\widetilde{\mathbf{L}}\widetilde{\mathbf{I}_\mathbf{d}}^{-1}(t)\widetilde{\mathbf{p}}(t) - \widetilde{\mathbf{p}}^T(t)\widetilde{\mathbf{I}_\mathbf{d}}^{-1}(t)\widetilde{\mathbf{L}}\widetilde{\mathbf{\Gamma}}(t), \\ &= -2\widetilde{\mathbf{\Gamma}}^T(t)\widetilde{\mathbf{L}}\widetilde{\mathbf{\Gamma}}(t), \end{aligned} \tag{4.20}$$

where $\widetilde{\mathbf{L}}$ is a symmetric positive semi-definite Laplacian matrix. Hence, $\dot{V}(\widetilde{\mathbf{p}}(t)) \leq 0$ holds for all $t \geq 0$. Since $V(\widetilde{\mathbf{p}}(t)) \geq 0$ (lower bounded) and $\dot{V}(\widetilde{\mathbf{p}}(t))$ is non-increasing, by Lemma 3.1, $V(\widetilde{\mathbf{p}}(t))$ converges to a limit as $t \to \infty$. This implies that $\widetilde{\mathbf{p}}(t)$ is bounded together with $\widetilde{\mathbf{\Gamma}}(t)$ and $\widetilde{\mathbf{I}_\mathbf{d}}(t)$.

Note that (4.20) can also be written as

$$\dot{V}(\widetilde{\mathbf{p}}(t)) = -2 \sum_{i \in \mathcal{M}\setminus\{0\}} \sum_{s \in \mathcal{U}_i} Z_i \Gamma_i^s(t)\big(\Gamma_i^s(t) - \Gamma_{i,ref}^s(t)\big), \tag{4.21}$$

whose time derivative can be expressed as

$$\ddot{V}(\widetilde{\mathbf{p}}(t)) = -2 \sum_{i \in \mathcal{M}\setminus\{0\}} \sum_{s \in \mathcal{U}_i} Z_i \Big[2\Gamma_i^s(t)\dot{\Gamma}_i^s(t) - \dot{\Gamma}_i^s(t)\Gamma_{i,ref}^s(t) - \Gamma_i^s(t)\dot{\Gamma}_{i,ref}^s(t)\Big]. \tag{4.22}$$

Using (4.5) and (4.15), $\dot{\Gamma}_i^s(t)$ can be calculated by

$$\begin{aligned}
\dot{\Gamma}_i^s(t) &= \frac{d}{dt}\left(\frac{p_i^s(t)}{I_{i,k}^s(t)}\right) = \frac{\dot{p}_i^s(t)I_{i,k}^s(t) - p_i^s(t)\dot{I}_{i,k}^s(t)}{{I_{i,k}^s}^2(t)} \\
&= \frac{1}{{I_{i,k}^s}^2(t)}\Big[-\beta_i^s Z_i\big(\Gamma_i^s(t) - \Gamma_{i,ref}^s(t)\big) - p_i^s(t)\dot{I}_{i,k}^s(t)\Big] \\
&= \frac{1}{{I_{i,k}^s}^2(t)}\Big[-\beta_i^s Z_i\big(\Gamma_i^s(t) - \Gamma_{i,ref}^s(t)\big) - p_i^s(t)\sum_{j\in\mathcal{M}\setminus i} h_{(i,j),k}^s \dot{p}_j^s(t)\Big] \\
&= -\beta_i^s Z_i \frac{\Gamma_i^s(t) - \Gamma_{i,ref}^s(t)}{{I_{i,k}^s}^2(t)} - \frac{p_i^s(t)}{{I_{i,k}^s}^2(t)} \sum_{j\in\mathcal{M}\setminus i} h_{(i,j),k}^s \beta_j^s \frac{{\Gamma_j^s}^2(t)}{p_j^s(t)} Z_j \left[1 - \frac{\Gamma_{j,ref}^s(t)}{\Gamma_j^s(t)}\right] \qquad (4.23)
\end{aligned}$$

Since it is already shown that $I_{m,k}^s(t)$, $p_m^s(t)$, $\beta_{m,k}^s$, $h_{(m,j),k}^s$ and $\Gamma_m^s(t)$ are bounded $\forall t \geq 0$, which implies $\Gamma_{m,ref}^s(t)$ is also bounded, $\dot{\Gamma}_m^s(t)$ is bounded $\forall t \geq 0$. Furthermore, we have $i, j \in \mathcal{M}\setminus\{0\}$, where $\mathcal{M}$ has a finite number of elements. Hence, $\ddot{V}(\widetilde{\mathbf{p}}(t))$ is bounded $\forall t \geq 0$. From Lemma 3.2, we can conclude that $\dot{V}(\widetilde{\mathbf{p}}(t)) \to 0$ as $t \to \infty$. In another words, we have

$$\lim_{t\to\infty} \widetilde{\mathbf{\Gamma}}^T(t)\widetilde{\mathbf{L}}\widetilde{\mathbf{\Gamma}}(t) = 0 \qquad (4.24)$$

which implies $\widetilde{\mathbf{L}}\widetilde{\mathbf{\Gamma}}(t) = 0$ when $t \to \infty$. Since the underlying graph of the communication network is assumed to be connected (Assumption 1), the Laplacian matrix $\widetilde{\mathbf{L}}$ has a simple eigenvalue at zero [26]. In that sense, $\dot{V}(\widetilde{\mathbf{p}}(t)) = 0$ implies $\dot{\widetilde{\mathbf{p}}}(t) = 0$ and we can conclude from (3.3) and (3.10) that $\widetilde{\Gamma}_i^{v^*} = \widetilde{\Gamma}_j^{w^*}$ holds $\forall v \in \mathcal{U}_i$, $\forall w \in \mathcal{U}_j$, and $\forall i, j \in \mathcal{M}\setminus\{0\}$. □

Remark 4. *As long as (4.13) is satisfied, with any finite choice of weights, the proposed power update algorithm, PUA-III given in (4.10), converges to a fair solution.*

4.4. Simulation Results of PUA-II and PUA-III

In this section, simulation studies regarding the proposed algorithms PUA-II and PUA-III are carried out by considering the network topology depicted in Figure 4.2, which shows the relative locations of all BSs and UEs. The setup consists of 8 FBSs, each having 3 randomly placed UEs. There also exists a single MBS with 3 UEs, which acts as a constant source of interference to all FUEs. All base stations are assumed to have access to the same

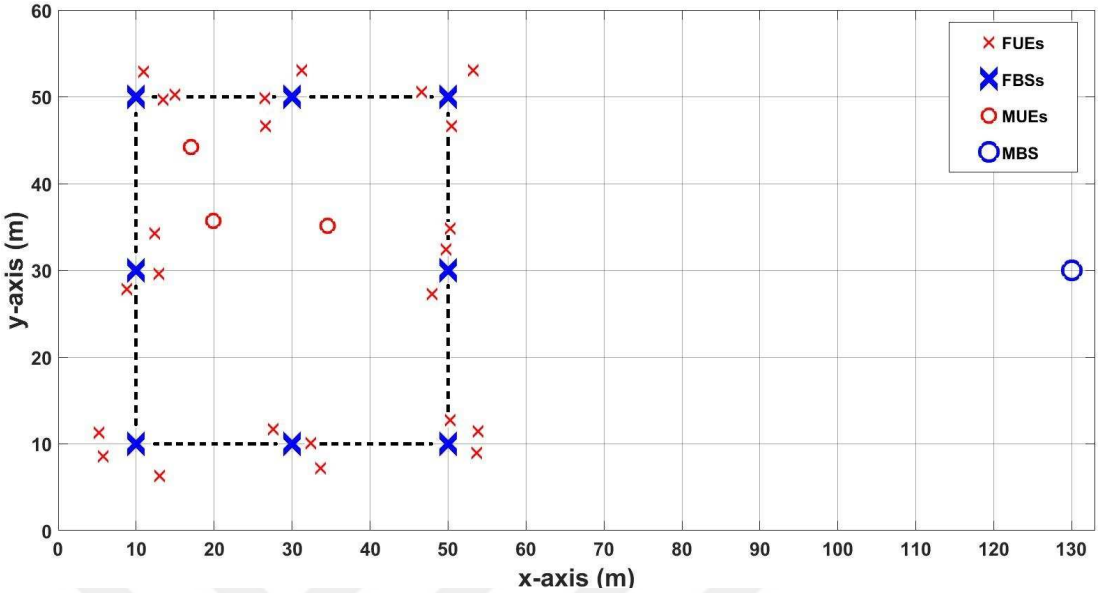

Figure 4.2. PUA-II and PUA-III simulation topology with edges.

$S = 3$ OFDMA subchannels. Dashed lines represent the communication links, on which the required information is carried between the FBSs. The collection of all dashed lines represents the underlying graph which is connected for this network. In simulations of PUA-III, specific weights are chosen according to (4.11), (4.12), and (4.13). Simulations of the algorithms are carried out by its discrete time implementation. By Euler's approximation, PUA-II and PUA-III (with given weight choices becomes (4.15)) can respectively be discretized as

$$p_m^s[k+1] = p_m^s[k] - T_s\beta_m^s\left[1 - \frac{\Gamma_{m,ref}^s[k]}{\Gamma_m^s[k]}\right]p_m^s[k], \tag{4.25}$$

and

$$p_m^s[k+1] = p_m^s[k] - T_s\beta_m^s Z_m\left[1 - \frac{\Gamma_{m,ref}^s[k]}{\Gamma_m^s[k]}\right]\frac{\Gamma_m^{s\,2}[k]}{p_m^s[k]}. \tag{4.26}$$

Here, sampling period T_s and update constant β_s^m are chosen same for all FBSs and subchannels. While simulating PUA-II and PUA-III, they are respectively chosen as $T_s\beta_m^s = 0.48s$ and $T_s\beta_m^s = 0.48\mu s$.

FBSs start executing the algorithm with randomly chosen initial power vector ($\widetilde{\mathbf{p}}[0]$), where all powers are less than 30 dBm (1 Watt). Transmission powers of MBS are randomly

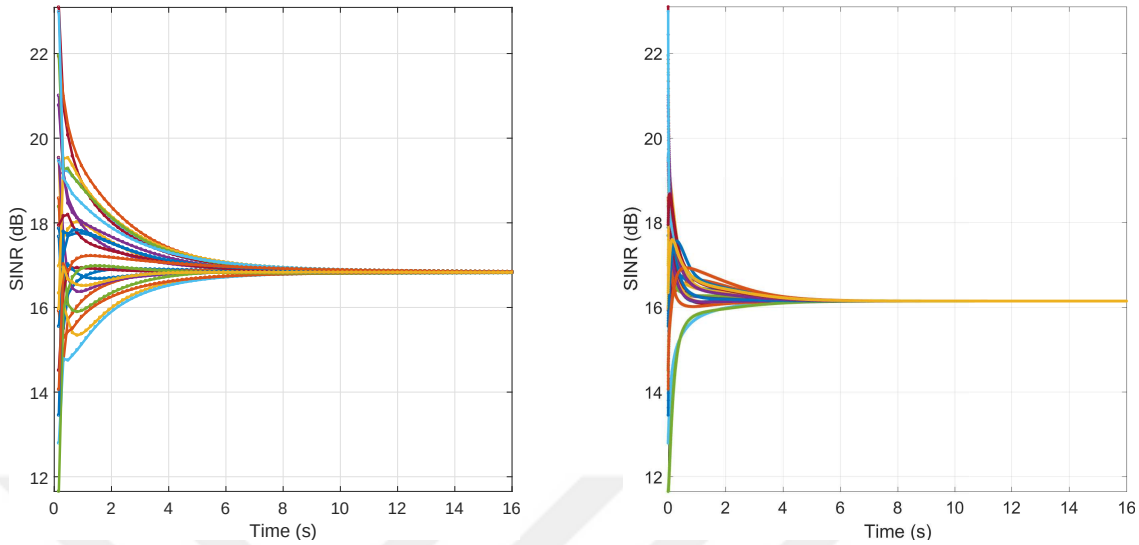

(a) Convergence of PUA-II (b) Convergence of PUA-III

Figure 4.3. Simulation results of PUA-II and PUA-III

chosen within the $43-50$ dBm ($20-100$ Watt) interval, where the thermal noise power is taken the same as -80 dBm (10^{-11} Watt) on all subchannels. Initial assignment of available subchannels are done randomly, and subchannel assignment is kept the same through the simulations. The channel gains are calculated by $g^s_{m,k} = \chi^{(s)} d^{-\alpha}_{m,k}$, where $d_{m,k}$ is the physical distance between BS m and UE k. $\chi^{(s)}$ value is generated randomly by Rayleigh distribution, and taken as [1.4127 1.0509 1.2092] for each subchannel. Path loss exponent is taken as $\alpha = 3$.

Simulation results of both algorithms (PUA-II and PUA-III) are given in Figure 4.3. As theoretically expected, at the end of each power update processes, all 24 FUEs reach consensus on a common SINR value. As a superiority of PUA-II over PUA-III, this final SINR value is found to be higher in PUA-II comparing to the PUA-III. Since the MBS is not a part of the underlaying communication graph of the topology given in Figure 4.2, SINR values of the MUEs are not expected to reach the consensus with the SINR values of FUEs. Therefore, they are not shown in Figure 4.3.

4.5. Chapter Summary

In this chapter, two new power update algorithms, namely PUA-II and PUA-III, are proposed for the OFDMA femtocell networks where each FBS can have more than one UE. It is analytically proven that both algorithms are capable of providing fairness when the underlying communication graph is connected. Theoretical studies are also illustrated with a numerical example. In terms of computational complexity, algorithms are easy to implement and the required exchange of information are kept minimal for both algorithms. In next chapter, we present two joint frequency/power update algorithms which can be considered as the optimized versions of PUA-II and PUA-III.

5. JOINT FREQUENCY/POWER UPDATE ALGORITHMS FOR OFMDA FEMTOCELL NETWORKS

In OFDMA femtocell networks, frequency allocation plays an important role in interference management and throughput maximization. In order to realize this importance, consider a simple network with 2 BS/UE pairs each having access to the same 2 OFDMA subchannels. When each UE gets service on the same subchannel, interference exposed by each UE can be dramatically dropped by a simple subchannel change, which also results in improved throughput. With a similar objective, by including frequency allocation in the power update algorithms proposed in Chapter 4, the final SINR value that every UE converges can be maximized.

In this chapter, we propose 2 suboptimal joint frequency/power update algorithms, namely JFPUA-I and JFPUA-II, which are respectively one step optimized versions of the PUA-II and PUA-III presented in Chapter 4. Each of these joint algorithms consists of consecutive usage of a frequency allocation phase and a power update part. In the frequency allocation part, each BS updates its frequency assignment vector by solving an integer programming problem. Then, the corresponding power update algorithm (PUA-II or PUA-III) runs for the remaining time.

As the chapter organization, first, some preliminary definitions will be given in Section 5.1. Then, some important results about the infeasibility of noise–free network are presented in Section 5.2. A frequency allocation scheme is derived in Section 5.3. Lastly, the joint algorithms and their simulation results will be given in Sections 5.4 and 5.5, respectively.

5.1. System Setup

Consider a femtocell network which is described in Section 4.1. When every active UE has the same SINR value γ^*, the following holds:

$$\Gamma^s_{m,k} = \rho^s_{m,k}\gamma^*, \tag{5.1}$$

where $\Gamma^s_{m,k}$ is either 0 or γ^* depending on if BS m serves UE k on subchannel s or not. When the fairness is achieved (i.e., $\Gamma^s_m = \gamma^*, \forall s \in \mathcal{U}, \forall m \in \mathcal{M} \setminus \{0\}$), by using (4.5) and (5.1), the following can be written:

$$\begin{aligned} p^s_m &= \gamma^* \sum_{k\in\mathcal{K}_m} \rho^s_{m,k}\left(\sum_{j\in\mathcal{M}\setminus m} h^s_{(m,j),k} p^s_j + \eta^s_{m,k} \right), \\ &= \gamma^* \sum_{k\in\mathcal{K}_m} \sum_{j\in\mathcal{M}\setminus m} \rho^s_{m,k} h^s_{(m,j),k} p^s_j + \gamma^* \sum_{k\in\mathcal{K}_m} \rho^s_{m,k}\eta^s_{m,k}, \\ &= \gamma^* \sum_{j\in\mathcal{M}\setminus m} p^s_j \sum_{k\in\mathcal{K}_m} \rho^s_{m,k} h^s_{(m,j),k} + \gamma^* \sum_{k\in\mathcal{K}_m} \rho^s_{m,k}\eta^s_{m,k}. \end{aligned} \tag{5.2}$$

In vector form, (5.2) can be represented as

$$\mathbf{p} = \mathbf{H}\mathbf{p}\gamma^* + \boldsymbol{\eta}\gamma^*. \tag{5.3}$$

Here, $\mathbf{p} = [p^{1^T}, p^{2^T}, \cdots, p^{S^T}]^T$ contains the transmission power information of the entire femtocell network where $p^s = [p^s_1, p^s_2, \cdots, p^s_{M_f}]^T$. Also the vector $\boldsymbol{\eta}$ contains the normalized noise values, and it is defined as $\boldsymbol{\eta} = [\eta^{1^T}, \eta^{2^T}, \cdots, \eta^{S^T}]^T$, where $\eta^s = [\eta^s_1, \eta^s_2, \cdots, \eta^s_{M_f}]^T$ and each η^s_i term can be calculated as

$$\eta^s_i = \sum_{k\in\mathcal{K}_i} \rho^s_{i,k}\eta^s_{i,k}. \tag{5.4}$$

Finally, the block diagonal square $\mathbf{H}$ matrix can be defined as

$$\mathbf{H} = \begin{bmatrix} \mathbf{H}^{(1)} & 0 & \dots & 0 \\ 0 & \mathbf{H}^{(2)} & \dots & \vdots \\ \vdots & \vdots & \ddots & 0 \\ 0 & \dots & 0 & \mathbf{H}^{(S)} \end{bmatrix}, \tag{5.5}$$

where $\mathbf{H}^{(s)} = [h_{ij}^{(s)}]$ is an $M_f \times M_f$ matrix with zero diagonal and non–negative elements on off–diagonals. Then, the entries of each off-diagonal $\mathbf{H}^{(s)}$ matrix can be defined as follows:

$$h_{ij}^{(s)} = \begin{cases} \sum\limits_{k \in \mathcal{K}_i} \rho_{i,k}^{s} h_{(i,j),k}^{s}, & \text{for } i \neq j \\ 0, & \text{otherwise} \end{cases} \tag{5.6}$$

With the definitions given above, some results about the infeasibility of the noise free network are given in the next section.

5.2. A Special Case: Noise Free System

When the thermal noise in the system is neglected (i.e., $\boldsymbol{\eta} = 0$), by dividing each side of (5.3) by γ^*, we obtain

$$\mathbf{H}\mathbf{p}^* = \tfrac{1}{\gamma^*}\mathbf{p}^*. \tag{5.7}$$

For a non-negative $M \times M$ matrix $\mathbf{A}$ to be irreducible, the necessary and sufficient condition is $(\mathbf{I}+\mathbf{A})^{M-1} > 0$ [31], where $\mathbf{I}$ is the identity matrix with appropriate size. Since $\mathbf{H}$ is a block diagonal matrix as described in (5.5), any power of $(\mathbf{I}+\mathbf{A})$ remains block diagonal. Hence, we can conclude that $\mathbf{H}$ is reducible, and the Perron–Frobenius theorem is inconclusive. However, by considering each off-diagonal $\mathbf{H}^{(s)}$ matrix individually, we can draw the following conclusion on the noise free system.

Theorem 5.1. *For the system described by (4.5), when the thermal noise is neglected (i.e., $\boldsymbol{\eta} = 0$), and all subchannels are assumed to be actively used by each BS, there is no feasible solution for (5.7) unless the spectral radius of $\mathbf{H}^{(s)}$ is the same for all s.*

Proof. When all subchannels are actively used, the following holds:

$$\sum_{k \in \mathcal{K}_i} \rho_{i,k}^{s} \neq 0, \forall s, \forall i \in \mathcal{I}. \tag{5.8}$$

Since $\mathbf{H}^{(s)}$ is non–negative and $\mathbf{H}^{(s)^n} > 0$ for all $n \geq 1$, as stated in Lemma 3.5, $\mathbf{H}^{(s)}$ is a primitive non–negative matrix for all $s \in \mathcal{S}$. Therefore, by Lemma 3.6, the following equation has its own unique feasible (γ^{s*}, p^{s*}) solution for each $s \in \mathcal{S}$:

$$\mathbf{H}^{(s)} p^{s*} = \frac{1}{\gamma^{s*}} p^{s*}, \tag{5.9}$$

where $\frac{1}{\gamma^{s*}} = r(\mathbf{H}^{(s)})$ and p^{s*} is the Perron eigenvector of $\mathbf{H}^{(s)}$. Since $\mathbf{H}$ is the block diagonal matrix defined by (5.5), for (5.7) to have a feasible solution, $\gamma^{s*} = \gamma^{\bar{s}*}$ should hold for all $s, \bar{s} \in \mathcal{S}$. □

Remark 5. *Since each $\mathbf{H}^{(s)}$ matrix is constructed by different channels gain ratios, the possibility of them having the same spectral radii can be considered as zero.*

Remark 6. *Theorem 5.1 states the infeasibility of the network under the assumption that all subchannels are actively used by each BS. This statement still holds for the relaxed assumption that each subchannel is actively used by at least one BS. Theorem* 8.3.1. *of [31] can be used to draw this conclusion.*

5.3. A Frequency Allocation Scheme

In this section, we derive a suboptimal frequency allocation scheme with the purpose of increasing the maximum achievable SINR in a given OFDMA femtocell network. Then, this scheme will be used jointly with PUA-II and PUA-III.

Consider a femtocell network which is described in Section 4.1. When every active UE has the same SINR value, (5.3) holds. Dividing each side by γ^*, (5.3) can be written as

$$\left(\frac{1}{\gamma^*}\mathbf{I}-\mathbf{H}\right)\mathbf{p}=\boldsymbol{\eta}. \tag{5.10}$$

In order to have a $\mathbf{p}\geq 0$ solution for all $\boldsymbol{\eta}\geq 0$, $\left(\frac{1}{\gamma^*}\mathbf{I}-\mathbf{H}\right)$ should be a monotone matrix. Since $\mathbf{H}$ has non–negative off–diagonal entries, being monotone for $\left(\frac{1}{\gamma^*}\mathbf{I}-\mathbf{H}\right)$ equivalently means being an M–matrix [27]. Hence, $\gamma^* < \frac{1}{r(\mathbf{H})}$ should hold, where $r(\mathbf{H})$ denotes the spectral radius of $\mathbf{H}$. The SINR value γ^* that every UE converges to has an upper limit of $\frac{1}{r(\mathbf{H})}$. Since $\mathbf{H}$ is made of the frequency assignment variables and channel gains, this upper limit can be improved by a proper frequency allocation scheme.

By Gersgorin disc theorem [31], the following holds for the spectral radius of the off–diagonal $\mathbf{H}^{(s)}$ matrix for all $s\in\mathcal{S}$:

$$r(\mathbf{H}^{(s)})\leq \max_i \sum_{j\neq i} h_{ij}^{(s)}. \tag{5.11}$$

Defining the diagonal matrix $\mathbf{D}^{(s)}=diag(p_1^s,p_2^s,\ldots,p_{M_f}^s)$, where $p_i^s>0$, the $\mathbf{H}^{(s)}$ matrix has the same eigenvalues as ${\mathbf{D}^{(s)}}^{-1}\mathbf{H}^{(s)}\mathbf{D}^{(s)}$ [31]. Hence, the largest Gersgorin disc defined in (5.11) can further be modified as

$$r(\mathbf{H}^{(s)})\leq \max_i \frac{1}{p_i^s}\sum_{j\neq i} h_{ij}^{(s)} p_j^s. \tag{5.12}$$

Since $\mathbf{H}$, given in (5.5), is a block diagonal matrix composed of $\mathbf{H}^{(s)}$ matrices, by using (5.6) and (5.12), $r(\mathbf{H})$ can be defined as

$$
\begin{aligned}
r(\mathbf{H}) &= \max_{s} r(\mathbf{H}^{(s)}) \\
&\leq \max_{s} \max_{i} \frac{1}{p_i^s} \sum_{j \neq i} h_{ij}^{(s)} p_j^s \\
&= \max_{s} \max_{i} \frac{1}{p_i^s} \sum_{j \neq i} p_j^s \sum_{k \in \mathcal{K}_i} \rho_{i,k}^s h_{(i,j),k}^s \\
&= \max_{s} \max_{i} \frac{1}{p_i^s} \sum_{j \neq i} \sum_{k \in \mathcal{K}_i} \rho_{i,k}^s h_{(i,j),k}^s p_j^s \\
&= \max_{s} \max_{i} \frac{1}{p_i^s} \sum_{k \in \mathcal{K}_i} \sum_{j \neq i} \rho_{i,k}^s h_{(i,j),k}^s p_j^s \\
&= \max_{s} \max_{i} \sum_{k \in \mathcal{K}_i} \rho_{i,k}^s \frac{1}{p_i^s} \sum_{j \neq i} h_{(i,j),k}^s p_j^s \\
&= \max_{i} \max_{s} \sum_{k \in \mathcal{K}_i} \rho_{i,k}^s \frac{1}{p_i^s} \sum_{j \neq i} h_{(i,j),k}^s p_j^s. \qquad (5.13)
\end{aligned}
$$

The proposed frequency allocation scheme is a discrete process which is performed synchronously by each BS prior to the power update. Z, which is a predefined even number, denoting the total number of iterations in frequency allocation scheme, all BSs set their transmission powers to the random levels at each of the odd–numbered iteration steps $z \in \{1,3,\ldots,Z-1\}$. Then, by using (4.5), we obtain

$$
\frac{1}{p_i^s[z]} \sum_{j \neq i} h_{(i,j),k}^s p_j^s[z] = \rho_{i,k}^s \frac{1}{\Gamma_{i,k}^s[z]} - \frac{\eta_{i,k}^s}{p_i^s[z]}, \qquad (5.14)
$$

where $\Gamma_{i,k}^s[z]$ denotes the SINR of the downlink signal transmitted by BS i to UE k on sub-channel s at iteration z. In order to find the expression on the left hand side of (5.14), we need to eliminate the unknown $\eta_{i,k}^s$ term. When each BS halves its transmission powers in the next iteration (i.e., $p_i^s[z+1] = \frac{p_i^s[z]}{2}$), (4.5) becomes

$$
\frac{1}{p_i^s[z]} \sum_{j \neq i} h_{(i,j),k}^s p_j^s[z] = \rho_{i,k}^s \frac{1}{\Gamma_{i,k}^s[z+1]} - \frac{2\eta_{i,k}^s}{p_i^s[z]}. \qquad (5.15)
$$

Using (5.14) and (5.15), the $\eta_{i,k}^s$ term can be eliminated, and the following is obtained:

$$
\frac{1}{p_i^s[z]} \sum_{j \neq i} h_{(i,j),k}^s p_j^s[z] = \rho_{i,k}^s \frac{2}{\Gamma_{i,k}^s[z]} - \rho_{i,k}^s \frac{1}{\Gamma_{i,k}^s[z+1]}. \qquad (5.16)
$$

Substituting (5.16) into (5.13), the spectral radius of the $\mathbf{H}$ matrix can be defined as

$$r(\mathbf{H}) \leq \max_i \max_s \sum_{k \in \mathcal{K}_i} \rho_{i,k}^s \left(\frac{2}{\Gamma_{i,k}^s[z]} - \frac{1}{\Gamma_{i,k}^s[z+1]} \right). \tag{5.17}$$

Note that an alternative scaling, such as $p_i^s[z+1] = c p_i^s[z]$ where $0 < c < 1$, can be utilized instead of halving the transmission powers.

Since $\gamma^* < \frac{1}{r(\mathbf{H})}$, the maximum achievable SINR γ^* can be maximized by minimizing $r(\mathbf{H})$. A so called pseudo–optimal solution for minimization of $r(\mathbf{H})$ can be achieved by reducing the upper bound of $r(\mathbf{H})$ defined in (5.17). Then, letting $f(\boldsymbol{\rho})$ denote this upper bound, the objective function that we want to minimize can be expressed as

$$f(\boldsymbol{\rho}) = \max_i \max_s \sum_{k \in \mathcal{K}_i} \rho_{i,k}^s \left(\frac{2}{\Gamma_{i,k}^s[z]} - \frac{1}{\Gamma_{i,k}^s[z+1]} \right). \tag{5.18}$$

With the required constraints, the optimization problem that needs to be solved after iteration $z+1$ is defined as follows:

$$\begin{aligned}
\underset{\boldsymbol{\rho}}{\text{minimize}} \quad & f(\boldsymbol{\rho}) = \max_i \max_s \sum_{k \in \mathcal{K}_i} \rho_{i,k}^s \left(\frac{2}{\Gamma_{i,k}^s[z]} - \frac{1}{\Gamma_{i,k}^s[z+1]} \right) && \text{(5.19a)} \\
\text{subject to} \quad & \sum_{k \in \mathcal{K}_i} \rho_{i,k}^s \leq 1, \ \ \forall i \in \mathcal{M} \setminus \{0\}, \forall s \in \mathcal{S}, && \text{(5.19b)} \\
& \sum_{s \in \mathcal{S}} \rho_{i,k}^s \leq 1, \ \ \forall i \in \mathcal{M} \setminus \{0\}, \forall k \in \mathcal{K}_i, && \text{(5.19c)} \\
& \rho_{i,k}^s \in \{0,1\}, \ \ k \in \mathcal{K}_i, \forall i \in \mathcal{M} \setminus \{0\}, \forall s \in \mathcal{S}, && \text{(5.19d)} \\
& p_i^s[z+1] = \frac{p_i^s[z]}{2}, \ \ \forall i \in \mathcal{M} \setminus \{0\}, \forall s \in \mathcal{S}, && \text{(5.19e)}
\end{aligned}$$

where constraint (5.19b) ensures that a BS can assign a subchannel to at most one UE. Constraint (5.19c) makes sure that a UE can be served on at most one subchannel. Also, by (5.19d), we specify that the decision variables can take binary values. Finally, constraint (5.19e), specifies that the transmission powers at iteration $z+1$ should be equal to the half of the transmission powers at iteration z.

The SINR of the downlink signal transmitted by BS i to UE k on subchannel s at iteration z is denoted by $\Gamma_{i,k}^{s}[z]$. Notice that, through an iteration step z, transmission powers on all subchannels remain the same even though the frequency allocation gets changed. Therefore, a frequency allocation change in BS $j \neq i$ does not affect the SINR of the UEs of BS i. In other words, $\Gamma_{i,k}^{s}[z]$ and $\Gamma_{i,k}^{s}[z+1]$ terms do not depend on the frequency allocation choice of the BS $j \neq i$. Also, the same subchannels are assumed to be available for every BS. Which means that the set of feasible solutions to problem (5.19), is actually a combination of set of identical feasible solutions for each BS. As a consequence of these facts, problem (5.19) can be partitioned into the individual subproblems. As an alternative to the centralized solution of the problem (5.19), each BS i solves its own subproblem in a distributed manner:

$$\underset{\rho_i}{\text{minimize}} \quad f_i(\rho_i) = \max_{s} \sum_{k \in \mathcal{K}_i} \rho_{i,k}^{s} \left(\frac{2}{\Gamma_{i,k}^{s}[z]} - \frac{1}{\Gamma_{i,k}^{s}[z+1]} \right) \tag{5.20a}$$

$$\text{subject to} \quad \sum_{k \in \mathcal{K}_i} \rho_{i,k}^{s} \leq 1, \ \ \forall s \in \mathcal{S}, \tag{5.20b}$$

$$\sum_{s \in \mathcal{S}} \rho_{i,k}^{s} \leq 1, \ \ \forall k \in \mathcal{K}_i, \tag{5.20c}$$

$$\rho_{i,k}^{s} \in \{0,1\}, \ \ k \in \mathcal{K}_i, \forall s \in \mathcal{S}, \tag{5.20d}$$

$$p_i^{s}[z+1] = \frac{p_i^{s}[z]}{2}, \ \ \forall s \in \mathcal{S}. \tag{5.20e}$$

In order to solve the problem defined in (5.20), BS i needs the SINR information of all of its UEs in all possible subchannel assignment scenarios at iterations z and $z+1$. Since FBSs are designed to serve up to 8 UEs [3], BS i can easily obtain $\Gamma_{i,k}^{s}[z]$ and $\Gamma_{i,k}^{s}[z+1]$ values for all $k \in \mathcal{K}_i, s \in \mathcal{S}$. The problem given in (5.20) is an integer programming problem with binary decision variables, various numerical tools such as [37] can be used to solve it.

Note that each BS sets its transmission powers to random values at odd–numbered iterations (i.e., $z \in \{1,3,\ldots,Z-1\}$), and halves them in the next even–numbered iteration $z+1$. After each even–numbered iteration step $z+1$ (i.e., $z \in \{1,3,\ldots,Z-1\}$), BSs solve their individual subproblems defined in (5.20). If the iteration $z+1$ results in a better objective value than the iteration $z-1$, BS i sets the solution of (5.20) at iteration $z+1$ as

its current frequency allocation vector ρ_i. Otherwise, BS i continues with the next iteration without changing its current frequency allocation vector. After Z iterations, where each BS has solved the problem (5.20) $Z/2$ times, the frequency allocation algorithm stops.

1: The network starts with random $\boldsymbol{\rho}[0]$ and $\mathbf{p}[0]$ vectors;
2: Set $f_i(\rho_i[0])$ to a large number, e.g. 10^6, for all i;
3: **for** $z := 1$ **to** $(Z-1)$ **step** 2 **do**
4: Each BS sets its transmission powers to the positive random values in the range of 0 to p_{max} (i.e., $0 < p_i^s[z] \leq p_{max}, \forall i, \forall s$);
5: For $\mathbf{p}[z]$, each BS i acquires SINR information $\Gamma_{i,k}^s[z]$ from its UEs for all possible subchannel assignments;
6: Each BS halves its transmission powers (i.e., $p_i^s[z+1] = \frac{p_i^s[z]}{2}, \forall i, \forall s$);
7: For $\mathbf{p}[z+1]$, each BS i acquires SINR information $\Gamma_{i,k}^s[z+1]$ from its UEs for all possible subchannel assignments;
8: Having $\Gamma_{i,k}^s[z]$ and $\Gamma_{i,k}^s[z+1]$ for all $k \in \mathcal{K}_i$ and $s \in \mathcal{S}$, each BS i finds the solution $\rho_i[z+1]$ to the problem (5.20);
9: **if** $f_i(\rho_i[z-1]) < f_i(\rho_i[z+1])$ **then**
10: $\rho_i[z+1] \leftarrow \rho_i[z-1]$;
11: **end if**
12: **end for**
13: $k \leftarrow 0$;
14: $\boldsymbol{\rho}[k] \leftarrow \boldsymbol{\rho}[Z]$;
15: $\boldsymbol{p}[k] \leftarrow \boldsymbol{p}[Z]$;
16: **repeat** with a proper sampling period T_s and fixed $\boldsymbol{\rho}[k]$
17: $p_m^s[k+1] \leftarrow p_m^s[k] - T_s \beta_m^s \left[1 - \frac{\Gamma_{m,ref}^s[k]}{\Gamma_m^s[k]}\right] p_m^s[k]$;
18: $k \leftarrow k+1$;
19: **until** $\mathbf{p}[k]$ converges

Figure 5.1. Joint Frequency/Power Update Algorithm I.

5.4. Joint Frequency/Power Update Algorithms (JFPUA-I and JFPUA-II)

In this section, we present 2 joint frequency/power update algorithms (JFPUA-I and JFPUA-II) for OFDMA femtocell networks. In terms of final SINR value that every UE converges, these algorithms are one step optimized versions of the power update algorithms proposed in Sections 4.2 and 4.3. The JFPUA-I and JFPUA-II are simply created by merging the frequency allocation scheme given in Section 5.3 with PUA-II and PUA-III, respectively.

Detailed description of the JFPUA-I is given in Figure 5.1. Since JFPUA-II differs from JFPUA-I only by line 17, it is not given as another figure. Instead, JFPUA-II can be obtained by replacing line 17 of JFPUA-I by (4.26). In both JFPUA-I and JFPUA-II, each FBS first updates its frequency allocation vector by solving the optimization problem defined in (5.20). Then, it executes the corresponding power update algorithm (PUA-II or PUA-III) for the remaining time.

As a natural extension of Theorems 4.1 and 4.2, the following corollary reveals the convergence properties of JFPUA-I and JFPUA-II:

Corollary 5.2. *Under Assumption 1, JFPUA-I and JFPUA-II converge to a fair solution* γ^**, where* $\Gamma_i{}^s = \gamma^*$ *holds for all* $i \in \mathcal{M} \setminus \{0\}$ *and* $s \in \mathcal{U}$.

Proof. Since PUA-II and PUA-III converge to a fair solution for all initial frequency assignment vectors, the proof directly follows from Theorems 4.1 and 4.2. □

5.5. Simulation Results of JFPUA-I and JFPUA-II

In this section, numerical analyses of the JFPUA-I and JFPUA-II are presented. The network topology used in the simulations is shown in Figure 4.2 where the locations of UEs are randomly changed for each trial. It is assumed that there exist 8 FBSs each serving 3 UEs where each FBS is assumed to have access to the same 3 OFDMA subchannels. The channel gains are calculated by $g^s_{m,k} = \chi^{(s)} d^{-\alpha}_{m,k}$, where $d_{m,k}$ is the physical distance between BS m and UE k. $\chi^{(s)}$ values are generated randomly before each trial. Also, the path loss exponent

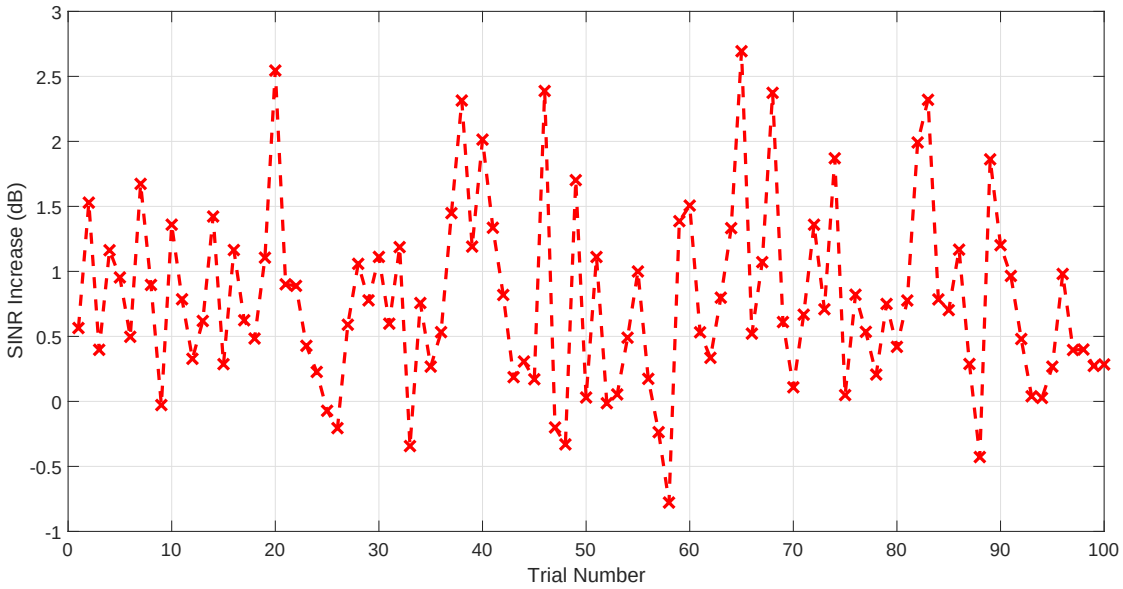

Figure 5.2. The outperformance of JFPUA-I relative to PUA-II

is taken as $\alpha = 3$. Since the channel gains and the FUE locations are changed randomly, different $\mathbf{H}$ matrices are used for each trial.

In the simulations, we first compared the performances of PUA-II and JFPUA-I in terms of the SINR value reached by consensus. Comparison of the algorithms are achieved by executing them on the identical networks. When this process is repeated 100 times, the results given in Figure 5.2 are obtained. The frequency allocation part of the joint algorithm is executed by 400 iterations (i.e., $Z = 400$). In the given 100 trials, JFPUA-I outperforms PUA-II 90 times, where the average SINR increase is calculated as $0.78dB$.

The effect of frequency allocation duration on the performance of JFPUA-I is also investigated in the numerical analyses. Starting with $Z = 2^1$, the iteration number is doubled until $Z = 2^9$. For each value of Z, JFPUA-I and PUA-II are compared 1000 times, and the average SINR outperformance of JFPUA-I is shown in Figure 5.3. On the average of 1000 random trials, the performance of JFPUA-I gets better while the iteration number Z in frequency allocation process is increasing. However, as Z increases, the performance of the joint algorithm seems to have diminishing returns which can be observed by looking at the slope of the curve.

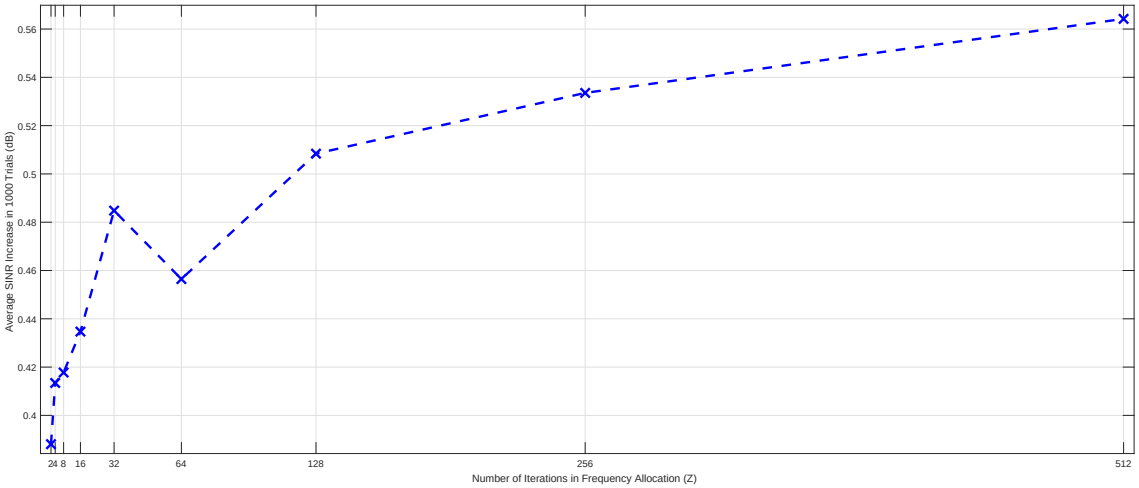

Figure 5.3. Performance of JFPUA-I with respect to the frequency allocation duration

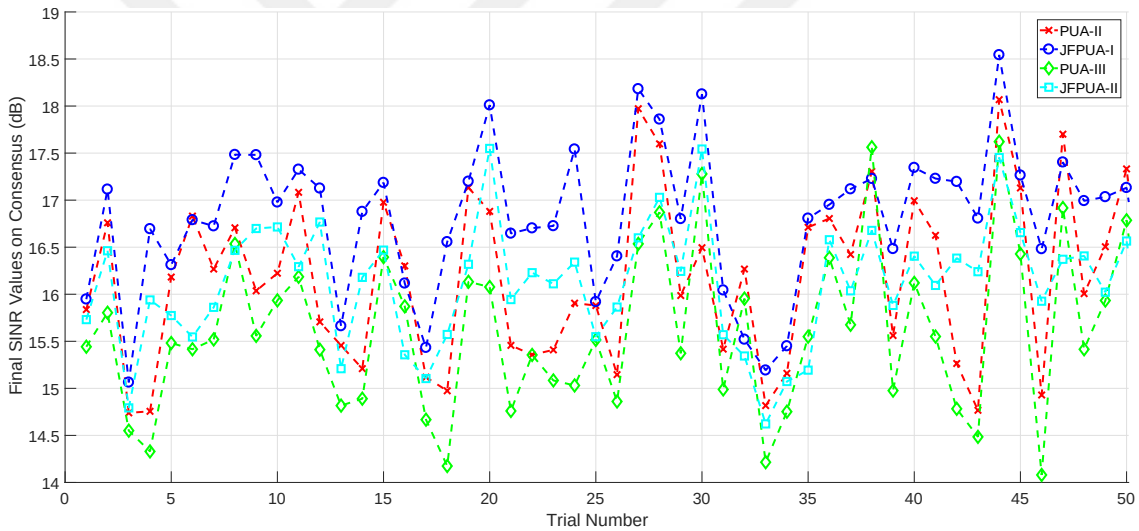

Figure 5.4. Performance comparison of PUA-II, JFPUA-I, PUA-III, and JFPUA-II

A more comprehensive simulation is carried out by running PUA-II, PUA-III, JFPUA-I and JFPUA-II 50 times on the identical networks with the same initial conditions. Figure 5.4 shows the results of these numerical analyses. Recall that JFPUA-I and JFPUA-II are respectively derived by merging PUA-II and PUA-III with the frequency allocation scheme given in (5.20a). Similar to the results given in Figure 5.2, JFPUA-II outperforms the PUA-III most of the times. It can also be seen in Figure 5.4 that, most of the times, JFPUA-I results in a higher consensus value compared to the other algorithms. Lastly, the superiority of PUA-II over PUA-III can also be observed in the figure.

5.6. Chapter Summary

In this chapter, OFDMA femtocell networks where FBSs may serve more than one UE are investigated. Under the SINR fairness constraint, it is shown that there is no feasible solution for the noise free systems. Then, in order to increase the maximum achievable SINR level, a frequency allocation scheme is proposed by using the Gersgorin disc theorem. Merging this scheme with the PUA-II and PUA-III, two joint frequency/power update algorithms (JFPUA-I and JFPUA-II) are proposed. Finally, the performances of these joint algorithms are illustrated with the numerical results.

6. CONCLUSION

In this thesis, power and frequency allocation problems in femtocell networks are studied. Some preliminary information about graph theory and consensus algorithms, along with the power control algorithms that constitute the basis of this thesis, are briefly discussed in the first chapter. Then, we propose an alternative (PUA-I) for the well known power control algorithm of Foschini–Miljanic. The PUA-I is theoretically and numerically shown to be converging to a fair solution by overcoming the infeasibility issue that was present in the algorithm of Foschini–Miljanic. Subsequently, PUA-I and the consensus based power control algorithm of Şenel–Akar are adapted for the OFDMA femtocell networks where base stations usually serve more than one user equipment. By theoretical and numerical analyses, it is shown that these new algorithms, namely PUA-II and PUA-III, ensure the convergence to a fair solution.

In order to increase the maximum achievable SINR in femtocell networks, a frequency allocation scheme, which is based on the Gersgorin disc theorem, is proposed. Then, the PUA-II and PUA-III are merged with this frequency allocation scheme for a higher convergence level, and two new joint frequency/power update algorithms (JFPUA-I and JFPUA-II) are proposed. By the numerical analyses, it is shown that the longer frequency allocation part leads to the better performance of the joint algorithms.

In the future studies, the proposed algorithms are planned to be studied for cases where the network model is time–varying in terms of the communication channels and topology. Also, there still is room for improvement of the frequency allocation scheme proposed. Finally, the power control in partially connected networks stands as an interesting problem to be studied.

REFERENCES

1. Ericsson, *Ericsson Mobility Report*, November 2018, `https://www.ericsson.com/assets/local/mobility-report/documents/2018/ericsson-mobility-report-november-2018.pdf`, accessed on Feb. 25, 2019.

2. Bendlin, R., V. Chandrasekhar, R. Chen, A. Ekpenyong and E. Onggosanusi, "From homogeneous to heterogeneous networks: A 3GPP Long Term Evolution rel. 8/9 case study", *45th Annual Conference on Information Sciences and Systems*, 2011.

3. Zhang, J. and G. D. l. Roche, *Femtocells: Technologies and Deployment*, Chichester, West Sussex, UK, Wiley, 2010.

4. Zahir, T., K. Arshad, A. Nakata and K. Moessner, "Interference Management in Femtocells", *IEEE Communications Surveys & Tutorials*, Vol. 15, No. 1, pp. 293–311, 2013.

5. Saquib, N., E. Hossain, L. B. Le and D. I. Kim, "Interference management in OFDMA femtocell networks: issues and approaches", *IEEE Wireless Communications*, Vol. 19, No. 3, pp. 86–95, 2012.

6. Lopez-Perez, D., A. Valcarce, G. D. L. Roche and J. Zhang, "OFDMA femtocells: A roadmap on interference avoidance", *IEEE Communications Magazine*, Vol. 47, No. 9, pp. 41–48, 2009.

7. Simsek, M., A. Czylwik, A. Galindo-Serrano and L. Giupponi, "Improved decentralized Q-learning algorithm for interference reduction in LTE-femtocells", *Wireless Advanced*, 2011.

8. Chandrasekhar, V. and J. Andrews, "Spectrum allocation in tiered cellular networks", *IEEE Transactions on Communications*, Vol. 57, No. 10, pp. 3059–3068, 2009.

9. Wu, Y., D. Zhang, H. Jiang and Y. Wu, "A novel spectrum arrangement scheme for femto

cell deployment in LTE macro cells", *IEEE 20th International Symposium on Personal, Indoor and Mobile Radio Communications*, 2009.

10. Kang, X., R. Zhang and M. Motani, "Price-Based Resource Allocation for Spectrum-Sharing Femtocell Networks: A Stackelberg Game Approach", *IEEE Journal on Selected Areas in Communications*, Vol. 30, No. 3, pp. 538–549, 2012.

11. Zhang, H., C. Jiang, N. C. Beaulieu, X. Chu, X. Wen and M. Tao, "Resource Allocation in Spectrum-Sharing OFDMA Femtocells With Heterogeneous Services", *IEEE Transactions on Communications*, Vol. 62, No. 7, pp. 2366–2377, 2014.

12. Ngo, D. T., S. Khakurel and T. Le-Ngoc, "Joint Subchannel Assignment and Power Allocation for OFDMA Femtocell Networks", *IEEE Transactions on Wireless Communications*, Vol. 13, No. 1, pp. 342–355, 2014.

13. Davaslioglu, K., C. C. Coskun and E. Ayanoglu, "New algorithms for maximizing cellular wireless network energy efficiency", *Information Theory and Applications Workshop (ITA)*, 2016.

14. Zhou, L., C. Zhu, R. Ruby, X. Wang, X. Ji, S. Wang and J. Wei, "QoS-aware energy-efficient resource allocation in OFDM-based heterogenous cellular networks", *International Journal of Communication Systems*, Vol. 30, No. 2, 2015.

15. Zahir, T., K. Arshad, Y. Ko and K. Moessner, "A downlink power control scheme for interference avoidance in femtocells", *7th International Wireless Communications and Mobile Computing Conference*, 2011.

16. Shen, Z., J. Andrews and B. Evans, "Adaptive resource allocation in multiuser OFDM systems with proportional rate constraints", *IEEE Transactions on Wireless Communications*, Vol. 4, No. 6, pp. 2726–2737, 2005.

17. Foschini, G. and Z. Miljanic, "A simple distributed autonomous power control algorithm and its convergence", *IEEE Transactions on Vehicular Technology*, Vol. 42, No. 4, pp.

641–646, 1993.

18. Senel, K. and M. Akar, “A Consensus-Based Coverage Algorithm For Self-Organizing Femtocell Networks”, *IEEE Communications Letters*, Vol. 20, No. 1, p. 141–144, 2016.

19. Senel, K. and M. Akar, “A Distributed Coverage Adjustment Algorithm for Femtocell Networks”, *IEEE Transactions on Vehicular Technology*, Vol. 66, No. 2, p. 1739–1747, 2017.

20. Senel, K. and M. Akar, “A fair downlink power control algorithm for femtocell networks”, *12th IEEE International Conference on Control and Automation (ICCA)*, 2016.

21. Senel, K. and M. Akar, “Performance analysis of a distributed power control algorithm for shared and split spectrum femtocell networks”, *Control Theory and Technology*, Vol. 14, No. 4, p. 314–322, 2016.

22. Ren, W., R. W. Beard and E. M. Atkins, “Information consensus in multivehicle cooperative control”, *IEEE Control Systems Magazine*, Vol. 27, No. 2, pp. 71–82, 2007.

23. Ren, W., “Consensus based formation control strategies for multi-vehicle systems”, *American Control Conference*, 2006.

24. Binetti, G., A. Davoudi, F. L. Lewis, D. Naso and B. Turchiano, “Distributed Consensus-Based Economic Dispatch With Transmission Losses”, *IEEE Transactions on Power Systems*, Vol. 29, No. 4, p. 1711–1720, 2014.

25. Zheng, Z., S. Xie, H. Dai, X. Chen and H. Wang, “An Overview of Blockchain Technology: Architecture, Consensus, and Future Trends”, *IEEE International Congress on Big Data (BigData Congress)*, 2017.

26. Olfati-Saber, R., J. A. Fax and R. M. Murray, “Consensus and cooperation in networked multi-agent systems”, *Proceedings of the IEEE*, Vol. 95, No. 1, pp. 215–233, 2007.

27. Plemmons, R., “M-matrix characterizations.I—nonsingular M-matrices”, *Linear Alge-*

bra and its Applications, Vol. 18, No. 2, pp. 175–188, 1977.

28. Zander, J., "Performance of optimum transmitter power control in cellular radio systems", *IEEE Transactions on Vehicular Technology*, Vol. 41, No. 1, p. 57–62, 1992.

29. Slotine, J.-J. E., W. Li *et al.*, *Applied nonlinear control*, Englewood Cliffs, NJ, Prentice Hall, 1991.

30. Ren, W. and R. W. Beard, *Distributed consensus in multi-vehicle cooperative control*, Springer, 2008.

31. Horn., R. A. and C. R. Johnson, *Matrix Analysis; 2nd Edition*, Cambridge University Press, 2013.

32. Boyle, M., *Notes on the Perron-Frobenius Theory of Nonnegative Matrices*, 2015, `https:pdfs.semanticscholar.org/2321/c0d2df3b3427e746ec8c43fa4f633c88fb9f.pdf`, accessed on Mar. 12, 2019.

33. Pillai, S., T. Suel and S. Cha, "The Perron-Frobenius theorem: Some of its applications", *IEEE Signal Processing Magazine*, Vol. 22, No. 2, p. 62–75, 2005.

34. Albrecht, J., "Minimal norms of nonnegative irreducible matrices", *Linear Algebra and its Applications*, Vol. 249, No. 1-3, p. 255–258, 1996.

35. Kincaid, D. R. and E. W. Cheney, *Numerical analysis: Mathematics of scientific computing*, American Mathematical Society, 2009.

36. Sevim, O. and M. Akar, "Consensus Based Power Update Algorithm for OFDMA-Based Femtocell Networks", *26th Mediterranean Conference on Control and Automation (MED)*, 2018.

37. Gleixner, A., L. Eifler, T. Gally, G. Gamrath, P. Gemander, R. L. Gottwald, G. Hendel, C. Hojny, T. Koch, M. Miltenberger, B. Müller, M. E. Pfetsch, C. Puchert, D. Rehfeldt, F. Schlösser, F. Serrano, Y. Shinano, J. M. Viernickel, S. Vigerske, D. Weninger, J. T.

Witt and J. Witzig, *The SCIP Optimization Suite 5.0*, Tech. rep., Optimization Online, December 2017.